

# Functional Genomics Reveals Extended Roles of the *Mycobacterium tuberculosis* Stress Response Factor $\sigma^{\text{HV}}$

Smriti Mehra<sup>1†</sup> and Deepak Kaushal<sup>1,2,3†\*</sup>

Division of Bacteriology and Parasitology, DNA Microarray and Expression Core, Tulane National Primate Research Center, Covington, Louisiana<sup>1</sup>; Department of Microbiology and Immunology, Tulane University School of Medicine, New Orleans, Louisiana<sup>2</sup>; and Joint Tulane-LSU Center for Experimental Infectious Disease Research, Louisiana State University School of Veterinary Medicine, Baton Rouge, Louisiana<sup>3</sup>

Received 17 January 2009/Accepted 7 April 2009

*Mycobacterium tuberculosis* is one of the most successful pathogens of humankind. During infection, *M. tuberculosis* must cope with and survive against a variety of different environmental conditions. Sigma factors likely facilitate the modulation of the pathogen's gene expression in response to changes in its extracellular milieu during infection.  $\sigma^{\text{H}}$ , an alternate sigma factor encoded by the *M. tuberculosis* genome, is induced by thiol-oxidative stress, heat shock, and phagocytosis. In response to these conditions,  $\sigma^{\text{H}}$  induces the expression of  $\sigma^{\text{B}}$ ,  $\sigma^{\text{E}}$ , and the thioredoxin regulon. In order to more effectively characterize the transcriptome controlled by  $\sigma^{\text{H}}$ , we studied the long-term effects of the induction of  $\sigma^{\text{H}}$  on global transcription in *M. tuberculosis*. The *M. tuberculosis* isogenic mutant of  $\sigma^{\text{H}}$  ( $\Delta\text{-}\sigma^{\text{H}}$ ) is more susceptible to diamide stress than wild-type *M. tuberculosis*. To study the long-term effects of  $\sigma^{\text{H}}$  induction, we exposed both strains to diamide, rapidly washed it away, and resumed culturing in diamide-free medium (post-diamide stress culturing). Analysis of the effects of  $\sigma^{\text{H}}$  induction in this experiment revealed a massive temporal programming of the *M. tuberculosis* transcriptome. Immediately after the induction of  $\sigma^{\text{H}}$ , genes belonging to the functional categories “virulence/detoxification” and “regulatory proteins” were induced in large numbers. Fewer genes belonging to the “lipid metabolism” category were induced, while a larger number of genes belonging to this category were down-regulated.  $\sigma^{\text{H}}$  caused the induction of the ATP-dependent *clp* proteolysis regulon, likely mediated by a transcription factor encoded by Rv2745c, several members of the *mce1* virulence regulon, and the sulfate acquisition/transport network.

Tuberculosis (TB) is responsible for over 2 million deaths annually (42). The failure of the BCG vaccine (1) and the emergence of drug-resistant strains of *Mycobacterium tuberculosis* have worsened this situation (34). To develop effective anti-TB drugs and vaccines, we need to define the mechanisms that help establish a long-term infection by *M. tuberculosis*.

Sigma ( $\sigma$ ) factors bind to the RNA polymerase and influence its promoter specificity (27). Most eubacteria contain a principal  $\sigma$  factor, which regulates the transcription of house-keeping genes. A variable number of alternate  $\sigma$  factors control responses to specific environmental stimuli, adaptation to stress, and bacterial virulence (35). The pathogenesis of TB involves multiple phases and is believed to involve a carefully deployed series of adaptive bacterial virulence factors. It is conceivable that temporal expression of specific regulons controlled by the induction or availability of one or more sigma factors (10, 13) allows *M. tuberculosis* to survive in multiple phases of the disease process (16). One such factor,  $\sigma^{\text{H}}$ , is induced after heat, redox, nitrosative, and acid stress (25, 30, 41, 45) and phagocytosis (16). Its activity is regulated in a redox-dependent manner by the antisigma factor RshA (50) as well as by the protein kinase PknB (38). An isogenic  $\Delta\text{-}\sigma^{\text{H}}$

mutant is attenuated in a mouse model and fails to induce typical pulmonary granulomatous pathology (25).  $\sigma^{\text{H}}$  directs the transcription of 31 genes, including those which encode extracytoplasmic function  $\sigma$  factors  $\sigma^{\text{E}}$  and  $\sigma^{\text{B}}$  and proteins involved in the maintenance of intrabacterial reducing capacity (25, 30). Expression of  $\sigma^{\text{H}}$  is induced after entry of *M. tuberculosis* into the host cells (19, 45), and this state of induced  $\sigma^{\text{H}}$  expression likely persists for a long period of time. Such continuing expression of  $\sigma^{\text{H}}$  must further affect gene expression in *M. tuberculosis*. The regulation of other transcription factors by  $\sigma^{\text{H}}$  creates a regulatory network with a potential for downstream modulation of gene expression. Induction of these proteins must in turn have further indirect impact on *M. tuberculosis* gene expression as a function of time. The study of these longer-term, enduring transcriptome changes will allow us to better understand the response of *M. tuberculosis* to phagocytosis and infection. We therefore sought to more clearly define these enduring effects of  $\sigma^{\text{H}}$ .

## MATERIALS AND METHODS

**Bacterial strains and culture conditions.** Wild-type *M. tuberculosis* and the  $\Delta\text{-}\sigma^{\text{H}}$  mutant were grown at 37°C in Middlebrook 7H9-albumin-dextrose-catalase-Tween 80-glycerol broth or 7H10-Dubos oleic acid complex-glycerol agar.

**Diamide stress.** We measured the effect of diamide on the viability of wild-type *M. tuberculosis* and  $\Delta\text{-}\sigma^{\text{H}}$  by the CFU method. Aliquots of cultures 1, 2, 3, and 4 h after addition of diamide were serially diluted and plated. These results were compared to those for the experiment where diamide was withdrawn after 1 h. Cultures grown to mid-log phase were exposed to 10 mM diamide for 1 h. The cultures were centrifuged (1,455 × g, 5 min), washed in diamide-free medium, and further cultured in an equal amount of this medium. These cultures were

\* Corresponding author. Mailing address: Division of Bacteriology and Parasitology, Tulane National Primate Research Center, 18703 Three Rivers Road, Covington, LA 70433. Phone: (985) 871-6254. Fax: (985) 871-6390. E-mail: dkaushal@tulane.edu.

† Both authors contributed equally to this work.

‡ Published ahead of print on 17 April 2009.

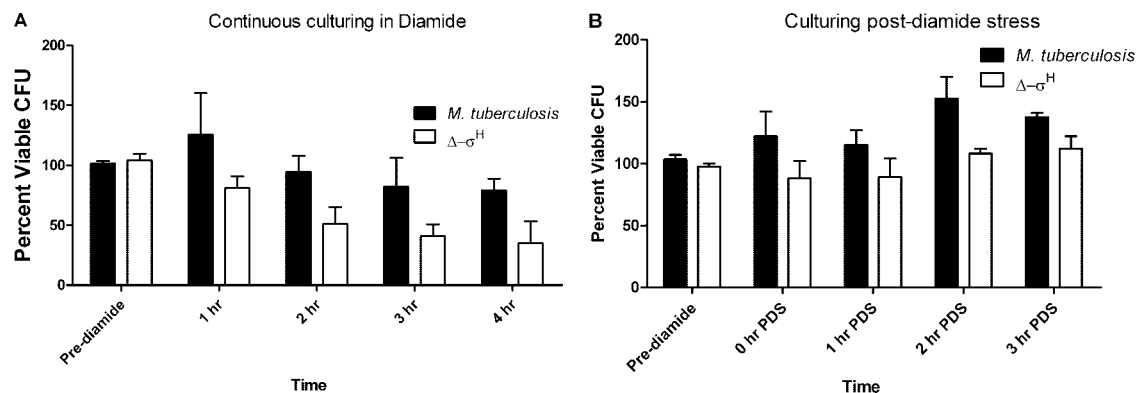


FIG. 1. Wild-type *M. tuberculosis* and the  $\Delta\text{-}\sigma^{\text{H}}$  mutant exhibit comparable inhibition levels PDS. Both wild-type *M. tuberculosis* and the  $\Delta\text{-}\sigma^{\text{H}}$  mutant were cultured in the presence of 10 mM diamide for 1, 2, 3, and 4 h (A) and 0 h (0 min), 1 h (60 min), 2 h (120 min), and 3 h (180 min) PDS (B). Data are means of results from three independent experiments, with plating for CFU performed in quadruplicates in each experiment, and the error bars represent standard deviations.

designated post-diamide stress (PDS) cultures. Aliquots obtained before diamide addition and at 0, 30, 60, 90, 120, and 180 min PDS were serially diluted and plated.

**Isolation of RNA.** RNA was isolated using the Trizol bead beater method (15), DNase treated, and purified (RNeasy; Qiagen) and its quantity assessed using a NanoDrop spectrophotometer.

**Microarray studies.** Whole-genome oligonucleotide microarrays representing ~4,750 *M. tuberculosis* open reading frames were obtained from the Pathogen Functional Genomic Resource Center (PFGRC) and used as recommended ([ftp://ftp.jcvi.org/pub/data/PFGRC/pdf\\_files/protocols/](ftp://ftp.jcvi.org/pub/data/PFGRC/pdf_files/protocols/)). Biological replicate hybridizations were performed using PDS samples from wild-type *M. tuberculosis* and the mutant. Spots with imperfect morphologies, low signal-to-noise ratios, saturated intensities, and high degrees of variability between replicates were excluded from the analysis. Data were analyzed using S<sup>+</sup> (Spotfire DecisionSite; TIBCO-Spotfire, Inc.) to determine statistically significant changes in expression, with adjustment for intensity bias by locally weighted scatter plot smoothing normalization (57). Genes were considered significantly and differentially expressed if they showed >1.75-fold changes with *P* values of <0.05.

**Reverse transcription and relative quantification of mRNA by quantitative PCR (qPCR).** Quantitative real-time reverse transcription-PCR was performed with cDNA corresponding to 50 ng RNA by using a SYBR green Supermix kit (Applied Biosystems) to interrogate the expression of  $\sigma^{\text{H}}$ ,  $\sigma^{\text{E}}$ ,  $\sigma^{\text{B}}$ , *trxB2*, *hsp*, *ctpG*, *bpoB*, *Rv2745c*, *clpP1*, and *mce1A*. Expression levels were normalized using  $\sigma^{\text{A}}$  as an invariant transcript, and the average relative expression levels were determined for four replicate experiments by using the following formula: (PDS level for wild-type *M. tuberculosis* – pre-diamide stress level for wild-type *M. tuberculosis*) – (PDS level for  $\Delta\text{-}\sigma^{\text{H}}$  – pre-diamide stress level for  $\Delta\text{-}\sigma^{\text{H}}$ ).

**Generation of rabbit polyclonal anti-Rv2745c antibody.** A predicted highly antigenic peptide sequence specific to the C terminus of the Rv2745c-encoded protein (VREVV GDVLR GARMS QGRTL REV-C) was used to immunize rabbits. The animals were boosted 4 and 6 weeks after prime immunization. Antisera were collected 2, 3, and 4 weeks after the final boost, titrated, and affinity purified. The antibody specifically recognized the product of the *M. tuberculosis* Rv2745c gene.

**Isolation of proteins, SDS-polyacrylamide gel electrophoresis, and Western blotting.** Total protein was isolated from 50 ml of each culture by using a B-PER (Pierce) kit. Sodium dodecyl sulfate (SDS)-polyacrylamide gel electrophoresis was performed on a 12% gel by using 20  $\mu\text{g}$  protein. The membrane was incubated with anti-Rv2745c antibody (1:1,000) and then with a goat anti-rabbit antibody (1:10,000) conjugated to horseradish peroxidase (Bio-Rad).

**Acetamide-induced expression of the *M. tuberculosis* Rv2745c gene.** The *M. tuberculosis* CDC1551 MT2816 (Rv2745c) gene was fused to the *Mycobacterium smegmatis* acetamidase promoter ( $P_{\text{ace}}$ ) on an integrative vector, pSCW38 (22). Following transformation of *M. tuberculosis*, the resulting strain (*M. tuberculosis*::pSM12) and its vector-only control (*M. tuberculosis*::pSCW38) were grown to log phase and induced with acetamide for 1 h. RNAs isolated from induced and uninduced cultures were used to perform qPCR as described earlier.

**Microarray data accession number.** Microarray data can be accessed from Gene Expression Omnibus (<http://www.ncbi.nlm.nih.gov/geo/>), using the provisional accession number GPL8382.

## RESULTS

**Wild-type *M. tuberculosis* and the  $\Delta\text{-}\sigma^{\text{H}}$  mutant exhibit comparable inhibition levels PDS.**  $\sigma^{\text{H}}$  protects *M. tuberculosis* from heat, oxidative, nitrosative, and acid stress conditions. The  $\Delta\text{-}\sigma^{\text{H}}$  mutant is more susceptible to diamide, a thiol-oxidative agent, which induces the expression of  $\sigma^{\text{H}}$  (30, 41). Prolonged culturing of the mutant in the presence of diamide would therefore lead to significant viability differences relative to wild-type *M. tuberculosis*, thus adversely affecting a global analysis of gene expression. When cultured continuously in the presence of diamide for 4 h, the viability of the  $\Delta\text{-}\sigma^{\text{H}}$  mutant was reduced by more than 50% relative to that of wild-type *M. tuberculosis* (Fig. 1A). Therefore, we devised an alternate strategy (PDS culturing) to study the long-term global effects of  $\sigma^{\text{H}}$  induction on the *M. tuberculosis* transcriptome. After 1 h, diamide was rapidly washed away and culturing resumed in normal, diamide-free medium. However, the viabilities of the two cultures remained comparable during the PDS culturing (Fig. 1B).

**Transcriptome comparison of wild-type *M. tuberculosis* and the  $\Delta\text{-}\sigma^{\text{H}}$  mutant PDS.** In order to verify that the expression of  $\sigma^{\text{H}}$  was induced during PDS culturing, we analyzed the presence of  $\sigma^{\text{H}}$ -specific transcripts at all PDS time points by using qPCR. As shown in Fig. 2A, expression of  $\sigma^{\text{H}}$  was induced at 0 min PDS in wild-type *M. tuberculosis* relative to that in the  $\Delta\text{-}\sigma^{\text{H}}$  mutant, peaked at 30 min PDS, and thereafter declined, reaching background levels by 120 min. Since the expressions of both  $\sigma^{\text{E}}$  and  $\sigma^{\text{B}}$  are known to be induced in a  $\sigma^{\text{H}}$ -dependent manner following diamide stress, we also analyzed the expressions of these genes in PDS samples. The expressions of both  $\sigma^{\text{E}}$  and  $\sigma^{\text{B}}$  were induced at 0 min PDS and remained at significantly high levels until the 30-min and 60-min PDS time points, respectively (Fig. 2A).

Wild-type *M. tuberculosis* transcripts made before diamide stress and at 0, 30, 60, 90, and 120 min PDS were then directly

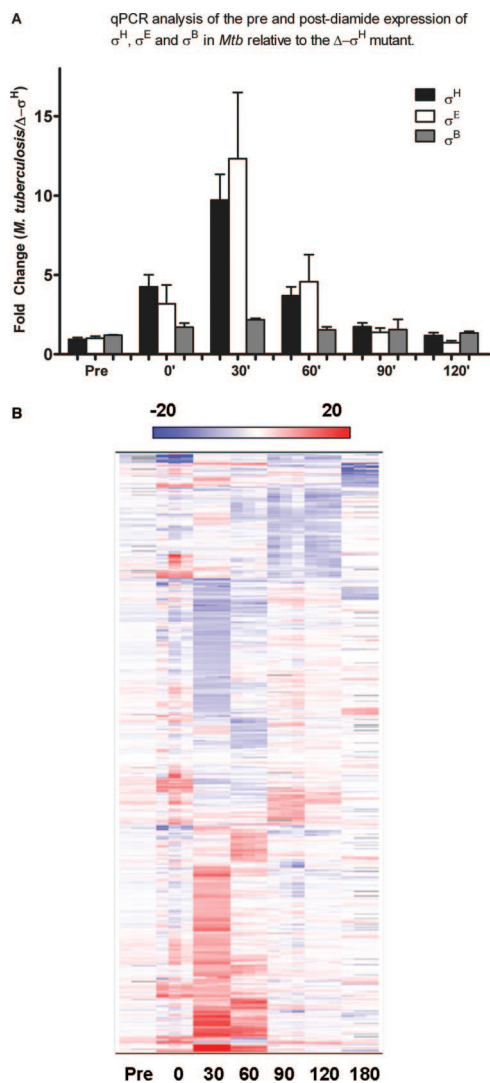


FIG. 2. Analysis of the comparative transcriptome levels of wild-type *M. tuberculosis* and the  $\Delta\text{-}\sigma^H$  mutant PDS. (A) The expression levels of  $\sigma^H$ ,  $\sigma^E$ , and  $\sigma^B$  in wild-type *M. tuberculosis* relative to the levels for the  $\Delta\text{-}\sigma^H$  mutant in PDS samples were assessed by qPCR at different time points. Values represent mean differences ( $n$ -fold)  $\pm$  standard deviations of results from quadruplicate experiments. (B) A two-dimensional clustering heat map shows *M. tuberculosis* genes expressed in a statistically significant manner for at least one PDS time point (0, 30, 60, 90, 120, or 180 min) relative to the pre-diamide induction time point. The intensity of the red color correlates with the degree of expression in wild-type *M. tuberculosis* relative to the level for the  $\Delta\text{-}\sigma^H$  mutant, while the intensity of the blue color correlates with the degree of expression in the mutant relative to the level for wild-type *M. tuberculosis*. For each time point, changes are shown for two distinct microarrays, each of which was hybridized to a biologically independent RNA sample, along with an average value.

compared to the  $\Delta\text{-}\sigma^H$  mutant transcripts by using microarrays. Figure 2B shows a hierarchical cluster of  $\sim 800$  genes differentially expressed significantly in the two strains for at least one of the PDS time points, vis-à-vis the pretreatment control. Forty-six genes were upregulated at 0 min PDS (Table 1), most of which were previously known to be dependent on  $\sigma^H$  for their expression (25, 30, 41). The expression of a much larger

number of genes was perturbed ( $\sim 380$  induced and  $\sim 340$  repressed) at the 30-min time point (see Tables 3 and 4). These substantial changes were perhaps due to the induction of  $\sigma^B$ ,  $\sigma^E$ , and several other transcription factors by  $\sigma^H$ . Each transcription factor in turn influences a distinct group of genes, leading to such profound global effects in gene expression. In contrast, 111 genes were induced and 120 repressed in wild-type *M. tuberculosis*, relative to the levels for the mutant, at 60 min PDS. The number of perturbed genes continued to decline with the passage of time. At 90 min PDS, 74 genes were induced and 32 genes repressed in wild-type *M. tuberculosis* relative to the levels for the mutant. At 120 min PDS, only 23 genes were induced. Clearly,  $\sigma^H$  continues to exert its influence on specific *M. tuberculosis* regulons, long after its initial induction. A detailed analysis of these interactions will enhance our understanding of the *M. tuberculosis* stress biology.

Many genes induced at 0 h PDS were known to be dependent on  $\sigma^H$  for their expression, e.g., the  $\sigma^H$ ,  $\sigma^B$ ,  $\sigma^E$ , *trxB2*, *trxC*, *groEL1*, *clpB*, *hsp*, *cysA1*, *cysT*, *cysW*, and Rv2466c genes (Table 1). These genes play important roles in maintaining cellular redox homeostasis, as peptidases or molecular chaperones, and in sulfate acquisition (52). Genes involved in molybdenum cofactor biosynthesis and transport and modulation of cell division were also induced. Genes with lower levels of expression in wild-type *M. tuberculosis* than in the mutant encode ABC transporters and DNA recombination or fatty acid biosynthesis proteins (Table 2). The expression levels of a majority of genes induced at 0 min PDS continued to be elevated at 30 min PDS, with the expression levels of  $\sigma^H$ ,  $\sigma^E$ ,  $\sigma^B$ , *trxB2*, *clpB*, and *hsp* peaking at this time point (Table 3). Other highly induced genes at this time point included *cadI*, CYP132 to CYP135A1, *lipL*, *lpqS*, *nuoF* to *nuoK*, *rubA*, *rubB*, Rv0303, Rv0331, Rv0692, Rv0790c, Rv1674c, Rv2348c, Rv2884, and Rv3753c. Many of these genes are known to be expressed under nonproliferating, microaerophilic conditions (55); starvation (5); antibiotic treatment (7); or phagocytosis (19, 45), indicating an overlap in the transcriptional programs of the pathogen in response to different stress conditions that mimic intraphagosomal stress. Genes induced in *M. tuberculosis* at this time were related to detoxification; stress; virulence; biosynthesis of molybdenum; transport of metal cations, RNA, sulfate/thiosulfate, and phosphate; and respiration (Table 3). The genes repressed in *M. tuberculosis* at this time were involved in biosynthesis of fatty acids, lipid virulence factors phiocerol mycocerosate and sulfolipid-1, polyketides, mycobactin siderophores, peptidoglycan, heme-porphyrin, and amino acids (Table 4) (56). The expression levels of the *mceI* operon, heat shock proteins, sulfate transporters, the thioredoxin regulon, and Rv2745c genes continued to be elevated in *M. tuberculosis* at 60 min PDS (Table 5). The expression of  $\sigma^H$  itself continued to be elevated (2.88-fold) but declined from its peak value at 30 min. Other genes induced in *M. tuberculosis* were involved in mycothiol-dependent detoxification; stress; fatty acid degradation; biosynthesis of phospholipids, cobalamin, and amino acids; immune-response/virulence; protein processing; energy metabolism; and macromolecule salvage (Table 5). Genes repressed in *M. tuberculosis* were involved in biosynthesis of fatty acids, phiocerol dimycocerosates, polyketides, glycoproteins, polysaccharides, proto-heme, and pantothenate and transport of phosphate, drugs, glycine

TABLE 1. Genes induced in wild-type *M. tuberculosis*, relative to the levels for the  $\Delta\text{-}\sigma^{\text{H}}$  mutant, at 0 min PDS<sup>a</sup>

Function	Locus tag	Gene	Fold expression		P
			Pre-diamide stress	0 min PDS	
Heat shock	Rv0384c	<i>clpB</i>	1.148 ± 0.043	3.760 ± 0.559	0.043
	Rv3417c	<i>groEL1</i>	1.051 ± 0.047	4.266 ± 0.768	0.049
	Rv3418c	<i>groES</i>	1.051 ± 0.047	2.562 ± 0.282	0.050
	Rv0251c	<i>hsp</i>	0.951 ± 0.048	2.141 ± 0.143	0.018
	Rv0350	<i>dnaK</i>	1.068 ± 0.004	2.902 ± 0.416	0.050
	Rv0469	<i>dnaJ1</i>	1.003 ± 0.026	2.607 ± 0.321	0.040
Transcription	Rv2710	<i>sigB</i>	0.998 ± 0.017	1.998 ± 0.159	0.042
	Rv1221	<i>sigE</i>	0.874 ± 0.0004	2.602 ± 0.392	0.050
	Rv3223c	<i>sigH</i>	0.869 ± 0.029	3.471 ± 0.502	0.045
	Rv0014c	<i>pknB</i>	0.926 ± 0.120	1.902 ± 0.111	0.002
	Rv1674c		1.056 ± 0.125	5.065 ± 0.181	0.003
Transport	Rv2397c	<i>cysA1</i>	0.944 ± 0.006	2.622 ± 0.324	0.043
	Rv2399c	<i>cysT</i>	0.831 ± 0.035	2.146 ± 0.229	0.043
	Rv2398c	<i>cysW</i>	1.110 ± 0.012	2.085 ± 0.139	0.035
	Rv1859	<i>modC</i>	1.208 ± 0.035	2.128 ± 0.239	0.049
	Rv0924c	<i>mntH</i>	0.909 ± 0.003	1.862 ± 0.196	0.046
	Rv1473		0.876 ± 0.003	1.774 ± 0.087	0.016
Detoxification	Rv2641	<i>cadI</i>	0.965 ± 0.016	4.139 ± 0.680	0.048
	Rv3913	<i>trxB2</i>	0.979 ± 0.018	4.550 ± 0.780	0.047
	Rv2899c	<i>fdhD</i>	1.234 ± 0.010	3.036 ± 0.310	0.039
Molybdopterin biosynthesis	Rv2453c	<i>mobA</i>	1.236 ± 0.025	3.301 ± 0.430	0.048
	Rv3206c	<i>moeB1</i>	1.095 ± 0.015	3.209 ± 0.018	0.003
Sulfate metabolism	Rv1336	<i>cysM</i>	0.914 ± 0.058	5.058 ± 0.173	0.006
	Rv1286	<i>cysN</i>	0.774 ± 0.246	3.511 ± 0.827	0.047

<sup>a</sup> The functional categorization of *M. tuberculosis* genes was based on their known functions as assigned by the TubercuList database (<http://genolist.pasteur.fr/TubercuList/>). For each gene, the changes in wild-type *M. tuberculosis* relative to the levels for the  $\Delta\text{-}\sigma^{\text{H}}$  mutant in the pre-diamide stress samples and the 0-min-PDS samples are shown, along with standard deviations. Statistical significance was assigned using the ANOVA function within the S<sup>+</sup> ArrayAnalyzer script.

betaine, sugar, and Mg<sup>2+</sup> (Table 6). The genes induced at 90 min PDS (Tables 7 and 8) were involved in biosynthesis of fatty acids, polyketides, the cell wall, molybdenum, polysaccharides, and thiosulfates; detoxification; transport of asparagine, cations, sulfate, phosphate, and drugs; DNA repair; protein processing; sensory regulation; and immune response. At 120 min PDS, global changes in gene expression had, to a large extent, subsided (Tables 9 and 10). These results should be interpreted in light of the fact that diamide-dependent expression of  $\sigma^{\text{H}}$  results in induction of  $\sigma^{\text{E}}$ ,  $\sigma^{\text{B}}$ , and several other transcription factors in wild-type *M. tuberculosis* relative to the level for the  $\Delta\text{-}\sigma^{\text{H}}$  mutant.

**Verification of microarray data.** To verify our transcriptome results, we performed SYBR green qPCR assays (Fig. 3A). The expression of *trxB2* was induced in wild-type *M. tuberculosis* relative to the level for the  $\Delta\text{-}\sigma^{\text{H}}$  mutant at 0 min PDS and remained at significantly high levels at all time points. The expression of *hsp* was induced at 0 min PDS and peaked at 30 min PDS. The expression of *ctpG* was induced only at the 30-min-PDS time point. The expression of *bpoB* was induced at both the 30 (peak)- and the 60-min-PDS time points, though its expression had been induced only at the earlier time point in microarray studies. The Rv2745c gene was induced between 30 and 90 min PDS, peaking at the 60-min time point. The expression of *clpP1* was induced as early as 0 min PDS and peaked at 60 min PDS. The expression of *mce1A* was induced at and peaked at 30 min PDS (Fig. 3A).

A polyclonal antibody against the Rv2745c-encoded transcription factor specifically detected the induced levels of this protein at 30, 60, and 90 min PDS only in wild-type *M. tuberculosis* (Fig. 3B). The corresponding band was not detected in comparable samples obtained from the  $\Delta\text{-}\sigma^{\text{H}}$  mutant. It has previously been reported that the expression of Rv2745c is controlled by  $\sigma^{\text{E}}$  (14, 51). The inability of the  $\Delta\text{-}\sigma^{\text{H}}$  mutant to induce the expression of  $\sigma^{\text{E}}$  likely results in the lack of induction of the Rv2745c gene.

**Conditional expression of the Rv2745c gene in *M. tuberculosis* induces the expression of the *clp* regulon.** The Rv2745c gene was cloned downstream of the *M. smegmatis* P<sub>acc</sub> in an integrative vector and used to transform *M. tuberculosis*. The conditional expression of Rv2745c gene was induced in this strain by adding acetamide at log phase. As measured by qPCR, the P<sub>acc</sub>-dependent expression of Rv2745c for 1 as well as 2 h led to high levels of induction of *clpP1*, *clpP2*, and *clpC1* (Fig. 4). Such induction was not observed in an *M. tuberculosis* strain transformed with a control vector, conclusively showing that the expression of the *M. tuberculosis* *clp* proteolysis regulon is controlled by the Rv2745c-encoded protein ClgR.

**Functional categorization of the wild-type *M. tuberculosis* PDS transcriptome relative to that for the  $\Delta\text{-}\sigma^{\text{H}}$  mutant.** The results obtained in this study were analyzed based on the *M. tuberculosis* genome functional categories. The ex-

TABLE 2. Genes repressed in wild-type *M. tuberculosis*, relative to the levels for the  $\Delta\text{-}\sigma^H$  mutant, at 0 min PDS<sup>a</sup>

Function	Locus tag	Gene	Fold expression		P
			Pre-diamide stress	0 min PDS	
Lipid metabolism	Rv0973c	<i>accA2</i>	1.206 ± 0.105	0.265 ± 0.061	0.039
	Rv0904c	<i>accD3</i>	1.059 ± 0.029	0.590 ± 0.058	0.041
	Rv3252c	<i>alkB</i>	1.427 ± 0.029	0.213 ± 0.041	0.013
	Rv2243	<i>fabD</i>	0.784 ± 0.062	0.357 ± 0.056	0.002
	Rv0859	<i>fadA</i>	1.548 ± 0.045	0.428 ± 0.193	0.047
	Rv2590	<i>fadD9</i>	0.985 ± 0.008	0.498 ± 0.111	0.047
	Rv3089	<i>fadD13</i>	0.965 ± 0.022	0.098 ± 0.005	0.004
	Rv0244c	<i>fadE5</i>	0.968 ± 0.036	0.229 ± 0.009	0.014
	Rv2724c	<i>fadE20</i>	1.261 ± 0.024	0.475 ± 0.102	0.036
	Rv0469	<i>umaA</i>	1.214 ± 0.008	0.567 ± 0.095	0.030
Intermediary metabolism	Rv3086	<i>adhD</i>	1.421 ± 0.187	0.049 ± 0.018	0.027
	Rv3841	<i>bfrB</i>	0.762 ± 0.002	0.182 ± 0.132	0.050
	Rv3617	<i>ephA</i>	0.961 ± 0.038	0.431 ± 0.063	0.043
	Rv3854c	<i>ethA</i>	0.844 ± 0.019	0.097 ± 0.016	0.00008
	Rv3251c	<i>rubA</i>	1.003 ± 0.051	0.161 ± 0.132	0.048
	Rv3250c	<i>rubB</i>	1.220 ± 0.059	0.175 ± 0.085	0.031
Cell wall associated	Rv0341	<i>iniB</i>	0.301 ± 0.163	0.294 ± 0.134	0.050
	Rv3084	<i>lipR</i>	1.412 ± 0.009	0.049 ± 0.028	0.006
	Rv1217c		1.120 ± 0.009	0.273 ± 0.054	0.011
	Rv2846c		0.908 ± 0.085	0.293 ± 0.083	0.035

<sup>a</sup> The functional categorization of *M. tuberculosis* genes was based on their known functions as assigned by the TubercuList database (<http://genolist.pasteur.fr/TubercuList/>). For each gene, the changes in wild-type *M. tuberculosis* relative to the levels for the  $\Delta\text{-}\sigma^H$  mutant in the pre-diamide stress samples and the 0-min-PDS samples are shown, along with standard deviations. Statistical significance was assigned using the ANOVA function within the  $S^+$  ArrayAnalyzer script.

pected number of genes in a given category was calculated for a given data set, based on the total number of genes assigned to each category in the genome. This was compared to the actual number of genes of each functional category induced or repressed at a given time point (Fig. 5A and B).

## DISCUSSION

The ability of *M. tuberculosis* to survive within the host requires resistance to various physiological and environmental stresses. Sigma factors encode a family of transcriptional regulators necessary for such adaptation processes. Expression of sigma factors  $\sigma^B$ ,  $\sigma^E$ , and  $\sigma^H$  has been shown to be required for the resistance of the pathogen to various environmental stresses likely to be encountered in vivo (25, 26, 29–31, 41). A subset of these sigma factors is induced during the growth of *M. tuberculosis* within macrophages (19) and required for virulence in animal models (2, 25, 30, 32). In this report, we shed more light on the complex transcriptional network controlled by  $\sigma^H$ . We interpreted these results in a global context by studying the relative abundances of genes belonging to a specific functional category. Initially (at 0 and 30 min PDS), and not unexpectedly, the expression levels of a larger-than-expected number of genes belonging to the virulence/detoxification category were upregulated in *M. tuberculosis*. Diamide is a thiol-oxidative agent. Detoxifying proteins Hsp, GroEL (which helps properly fold proteins) (52), ClpB and HtpX (peptidases) (52), SodA (which destroys free radicals toxic to *M. tuberculosis*) (11), and BpoB (which controls damaging reactive oxygen species during phagocytosis) are induced to likely help the pathogen effectively deal with the consequences of such stress. Initial oxidative damage by the host macrophages may serve as an environmental cue for *M. tuberculosis* to turn on the

expression of key virulence genes, which may in turn allow the pathogen to invade secondary cells and adapt to the host. Virulence genes induced by *M. tuberculosis* immediately following diamide stress include members of the *mce1* operon (49); Rv2525c, a substrate of the twin-arginine translocation system, which exports folded proteins (47); Rv1740, Rv2526, Rv2547, Rv2595, and Rv2829c, PIN domain antitoxins (3); CspA, an RNA chaperone that interacts with TA networks (58); and invasins, involved in interaction with phagocytes. However, fewer than the expected number of “lipid metabolism” genes were induced at 0 and 30 min PDS (Fig. 5A). This represents a marked shift in the metabolic profile of the pathogen immediately after phagocytosis. By silencing expensive functions at a time when it is faced with a high degree of potentially destructive stress, *M. tuberculosis* appears to conserve cellular energy and protect its lipids and mycolic acids from oxidative damage. Further reinforcing this point, the expression levels of more than the expected number of “lipid metabolism” genes, including those involved in mycolic acid synthesis, biogenesis of mycobactin siderophores, and lipid virulence factors, were repressed at 0 and 30 min PDS (Fig. 5B). Beyond 60 min PDS, the expression levels of more than the expected number of “intermediary metabolism” genes were upregulated in *M. tuberculosis*. This represents an adaptation from the initial “stress defense” mode to one where the pathogen prepares metabolites for the subsequent replication and proliferation. These genes are involved in arginine biosynthesis, macromolecular salvage, and protein processing. It is energetically more expensive for *M. tuberculosis* to biosynthesize L-arginine than for this organism to acquire it from the external environment (17, 54). That *M. tuberculosis* still synthesizes arginine reflects its inability to sequester it following oxidative stress. An increased need for protein processing and turnover

TABLE 3. Genes induced in wild-type *M. tuberculosis*, relative to the levels for the  $\Delta\text{-}\sigma^H$  mutant, at 30 min PDS<sup>a</sup>

Function	Locus tag	Gene	Fold expression		P	
			Pre-diamide stress	30 min PDS		
Heat shock	Rv0384c	<i>clpB</i>	1.148 ± 0.043	21.896 ± 0.344	0.004	
	Rv3417c	<i>groEL1</i>	1.051 ± 0.020	1.831 ± 0.037	0.003	
	Rv0440	<i>groEL2</i>	1.075 ± 0.0003	1.799 ± 0.158	0.049	
	Rv3418c	<i>groES</i>	1.342 ± 0.003	1.680 ± 0.100	0.067	
	Rv0351	<i>grpE</i>	1.057 ± 0.005	2.939 ± 0.074	0.008	
	Rv0251c	<i>hsp</i>	0.951 ± 0.048	20.969 ± 0.201	0.002	
	Rv0353	<i>hspR</i>	0.977 ± 0.007	3.491 ± 0.088	0.007	
	Rv0563	<i>hspX</i>	0.915 ± 0.027	1.840 ± 0.005	0.005	
	Rv0469	<i>dnaJ1</i>	1.003 ± 0.026	1.638 ± 0.030	0.002	
	Rv0250c		1.352 ± 0.470	16.275 ± 1.063	0.008	
Virulence/detoxification	MT1966	<i>aceA2</i>	1.366 ± 0.002	1.900 ± 0.065	0.025	
	Rv1123c	<i>bpoB</i>	1.017 ± 0.060	2.404 ± 0.100	0.003	
	Rv2641	<i>cadI</i>	0.965 ± 0.060	4.698 ± 0.464	0.026	
	Rv3648c	<i>cspA</i>	0.954 ± 0.006	2.588 ± 0.092	0.011	
	Rv3874	<i>esxB</i>	0.993 ± 0.035	1.799 ± 0.159	0.051	
	Rv3890c	<i>esxC</i>	1.045 ± 0.010	1.763 ± 0.002	0.002	
	Rv3891c	<i>esxD</i>	0.907 ± 0.011	2.786 ± 0.083	0.008	
	Rv3017c	<i>esxQ</i>	1.061 ± 0.035	2.804 ± 0.054	0.002	
	MT3105	<i>esxS</i>	0.855 ± 0.007	3.564 ± 0.159	0.013	
	Rv0169	<i>mce1A</i>	0.763 ± 0.013	2.924 ± 0.010	0.0003	
	Rv0170	<i>mce1B</i>	1.055 ± 0.015	1.766 ± 0.041	0.017	
	Rv0171	<i>mce1C</i>	1.016 ± 0.006	2.290 ± 0.052	0.010	
	Rv0172	<i>mce1D</i>	1.023 ± 0.009	1.780 ± 0.124	0.039	
	Rv0173	<i>mce1E (lprK)</i>	1.110 ± 0.009	2.505 ± 0.295	0.050	
	Rv0174	<i>mce1F</i>	1.005 ± 0.013	1.750 ± 0.020	0.010	
	Rv3846	<i>sodA</i>	1.344 ± 0.135	3.484 ± 0.338	0.049	
	Rv1471	<i>trxB1</i>	0.986 ± 0.019	46.508 ± 1.171	0.005	
	Rv3913	<i>trxB2</i>	0.979 ± 0.012	21.066 ± 0.647	0.007	
	Rv3914	<i>trxC</i>	1.214 ± 0.303	24.457 ± 0.204	0.004	
	Rv2525c		1.167 ± 0.002	3.111 ± 0.172	0.020	
	Rv1740		0.817 ± 0.019	2.590 ± 0.166	0.023	
	Rv2595		0.795 ± 0.011	2.505 ± 0.128	0.015	
	Rv2829c		1.131 ± 0.026	2.342 ± 0.039	0.012	
	Rv0660c		0.757 ± 0.026	2.048 ± 0.078	0.018	
	Rv2547		0.770 ± 0.015	1.908 ± 0.007	0.004	
	Rv2526		0.772 ± 0.013	1.853 ± 0.038	0.032	
	Rv2526		0.772 ± 0.013	1.853 ± 0.038	0.032	
	Transcription	Rv2745c	<i>clgR</i>	1.015 ± 0.061	5.495 ± 0.903	0.042
		Rv1994c	<i>cmtR</i>	0.929 ± 0.021	6.574 ± 0.641	0.024
		Rv1909c	<i>furA</i>	1.289 ± 0.059	3.610 ± 0.051	0.010
Rv2711		<i>ideR</i>	1.026 ± 0.007	3.610 ± 0.114	0.009	
Rv3291c		<i>lprA</i>	1.119 ± 0.016	3.072 ± 0.194	0.020	
Rv0981		<i>mprA</i>	1.157 ± 0.017	2.360 ± 0.016	0.0002	
Rv2710		<i>sigB</i>	1.255 ± 0.017	2.541 ± 0.030	0.008	
Rv3414c		<i>sigD</i>	1.174 ± 0.041	1.832 ± 0.015	0.019	
Rv1221		<i>sigE</i>	0.874 ± 0.0004	19.133 ± 0.236	0.002	
Rv3223c		<i>sigH</i>	0.870 ± 0.029	5.883 ± 0.013	0.0007	
Rv3911		<i>sigM</i>	0.994 ± 0.009	1.907 ± 0.102	0.027	
Rv3232c		<i>pvdS</i>	0.928 ± 0.020	2.163 ± 0.206	0.033	
Rv2358		<i>zurR</i>	0.736 ± 0.044	1.977 ± 0.114	0.012	
Rv1674c			1.056 ± 0.125	6.603 ± 0.400	0.021	
Rv2884			0.660 ± 0.059	4.062 ± 0.131	0.012	
Rv3295			1.017 ± 0.037	3.167 ± 0.138	0.018	
Rv3291c			1.119 ± 0.016	3.072 ± 0.194	0.020	
Cell wall associated		Rv0835	<i>lpqQ</i>	0.944 ± 0.097	2.707 ± 0.068	0.021
	Rv0847	<i>lpqS</i>	1.066 ± 0.088	5.901 ± 0.423	0.023	
	Rv1252c	<i>lprE</i>	1.591 ± 0.020	2.607 ± 0.048	0.015	
	Rv1541c	<i>lprI</i>	0.936 ± 0.011	2.433 ± 0.038	0.004	
	Rv1899c	<i>lppD</i>	1.310 ± 0.063	2.219 ± 0.086	0.005	
	Rv2080	<i>lppJ</i>	1.175 ± 0.022	2.567 ± 0.057	0.012	
	Rv1338	<i>murI</i>	0.746 ± 0.050	6.006 ± 0.378	0.018	
	Rv3810	<i>pirG</i>	1.396 ± 0.004	2.750 ± 0.111	0.017	

Continued on following page

TABLE 3—Continued

Function	Locus tag	Gene	Fold expression		P
			Pre-diamide stress	30 min PDS	
Transport	Rv1992c	<i>ctpG</i>	0.916 ± 0.060	3.355 ± 0.134	0.006
	Rv2397c	<i>cysA1</i>	0.944 ± 0.006	2.962 ± 0.106	0.011
	Rv2399c	<i>cysT</i>	0.831 ± 0.035	2.893 ± 0.192	0.024
	Rv0655	<i>mkl</i>	1.092 ± 0.035	2.021 ± 0.054	0.014
	Rv2400c	<i>subI</i>	1.386 ± 0.028	2.889 ± 0.235	0.039
	MT0955	<i>pstS1</i>	1.693 ± 0.007	2.485 ± 0.042	0.014
	Rv1668c		0.977 ± 0.035	2.171 ± 0.013	0.004
	Rv2477c		1.032 ± 0.035	2.067 ± 0.035	0.0006
Sulfate metabolism	Rv1286	<i>cysCN</i>	0.778 ± 0.246	2.924 ± 0.008	0.025
	Rv1285	<i>cysD</i>	1.115 ± 0.100	6.483 ± 0.162	0.001
	Rv2335	<i>cysE</i>	0.854 ± 0.124	1.817 ± 0.019	0.024
	Rv0848	<i>cysK2</i>	0.842 ± 0.072	11.028 ± 1.308	0.027
	Rv1336	<i>cysM</i>	0.914 ± 0.058	11.442 ± 0.094	0.0007
	Rv1335	<i>cysO</i>	0.925 ± 0.003	6.606 ± 0.183	0.007
	Hypothetical proteins	Rv2466c		1.161 ± 0.004	39.813 ± 0.476
Rv0140			1.362 ± 0.006	30.307 ± 6.028	0.046
Rv3463			0.996 ± 0.016	26.869 ± 0.082	0.0005
MT3140			1.151 ± 0.032	24.694 ± 1.428	0.013

<sup>a</sup> The functional categorization of *M. tuberculosis* genes was based on their known functions as assigned by the TubercuList database (<http://genolist.pasteur.fr/TubercuList/>). For each gene, the changes in wild-type *M. tuberculosis* relative to the levels for the  $\Delta\sigma^H$  mutant in the pre-diamide stress samples and the 30-min-PDS samples are shown, along with standard deviations. Statistical significance was assigned using the ANOVA function within the S<sup>+</sup> ArrayAnalyzer script.

may be necessitated due to damage to protein structure by oxidative stress and a subsequent inability of the heat shock network to completely restore the structures of damaged proteins. Such proteins may need to be completely degraded via the ATP-dependent *clp* proteolytic pathway. At 60 min PDS, the “lipid metabolism” category continued to be repressed in *M. tuberculosis* (Fig. 5B). The 90-min-PDS time point marked

a significant shift in the pattern of wild-type *M. tuberculosis* gene expression relative to the level for the  $\Delta\sigma^H$  mutant. At both 90 and 120 min PDS, the expression levels of a large number of “lipid metabolism” and “cell wall-associated” genes were elevated. This included many genes whose expression levels were initially repressed. A larger-than-expected number of “lipid metabolism” genes were no longer repressed. This

TABLE 4. Genes repressed in wild-type *M. tuberculosis*, relative to the levels for the  $\Delta\sigma^H$  mutant, at 30 min PDS<sup>a</sup>

Function	Locus tag	Gene	Fold expression		P	
			Pre-diamide stress	30 min PDS		
Lipid metabolism	Rv0973c	<i>accA2</i>	1.206 ± 0.105	0.265 ± 0.061	0.039	
	Rv0904c	<i>accD3</i>	1.059 ± 0.029	0.590 ± 0.058	0.041	
	Rv3252c	<i>alkB</i>	1.427 ± 0.029	0.213 ± 0.041	0.013	
	Rv2243	<i>fabD</i>	0.784 ± 0.062	0.357 ± 0.056	0.002	
	Rv0859	<i>fadA</i>	1.548 ± 0.045	0.428 ± 0.193	0.047	
	Rv2590	<i>fadD9</i>	0.985 ± 0.008	0.498 ± 0.111	0.047	
	Rv3089	<i>fadD13</i>	0.965 ± 0.022	0.098 ± 0.005	0.004	
	Rv0244c	<i>fadE5</i>	0.968 ± 0.036	0.229 ± 0.009	0.014	
	Rv2724c	<i>fadE20</i>	1.261 ± 0.024	0.475 ± 0.102	0.036	
	Rv0469	<i>umaA</i>	1.214 ± 0.008	0.567 ± 0.095	0.030	
	Intermediary metabolism	Rv3086	<i>adhD</i>	1.421 ± 0.187	0.049 ± 0.018	0.027
		Rv3841	<i>bfrB</i>	0.762 ± 0.002	0.182 ± 0.132	0.050
		Rv3617	<i>ephA</i>	0.961 ± 0.038	0.431 ± 0.063	0.043
Rv3854c		<i>ethA</i>	0.844 ± 0.019	0.097 ± 0.016	0.00008	
Rv3251c		<i>rubA</i>	1.003 ± 0.051	0.161 ± 0.132	0.048	
Rv3250c		<i>rubB</i>	1.220 ± 0.059	0.175 ± 0.085	0.031	
Cell wall associated	Rv0341	<i>iniB</i>	0.301 ± 0.163	0.294 ± 0.134	0.050	
	Rv3084	<i>lipR</i>	1.412 ± 0.009	0.049 ± 0.028	0.006	
	Rv1217c		1.120 ± 0.009	0.273 ± 0.054	0.011	
	Rv2846c		0.908 ± 0.085	0.293 ± 0.083	0.035	

<sup>a</sup> The functional categorization of *M. tuberculosis* genes was based on their known functions as assigned by the TubercuList database (<http://genolist.pasteur.fr/TubercuList/>). For each gene, the changes in wild-type *M. tuberculosis* relative to the levels for the  $\Delta\sigma^H$  mutant in the pre-diamide stress samples and the 30-min-PDS samples are shown, along with standard deviations. Statistical significance was assigned using the ANOVA function within the S<sup>+</sup> ArrayAnalyzer script.

TABLE 5. Genes induced in wild-type *M. tuberculosis*, relative to the levels for the  $\Delta\text{-}\sigma^H$  mutant, at 60 min PDS<sup>a</sup>

Function	Locus tag	Gene	Fold expression		P
			Pre-diamide stress	60 min PDS	
Heat shock	Rv0384c	<i>clpB</i>	1.148 ± 0.043	5.072 ± 0.851	0.050
	Rv0351	<i>grpE</i>	1.0571 ± 0.005	3.721 ± 0.363	0.031
	Rv0353	<i>hspR</i>	0.977 ± 0.007	4.653 ± 0.521	0.031
	Rv0352	<i>dnaJ1</i>	1.003 ± 0.026	10.429 ± 1.595	0.038
	Rv2373c	<i>dnaJ2</i>	0.851 ± 0.011	1.992 ± 0.186	0.034
	Rv3417c	<i>groEL1</i>	1.051 ± 0.047	6.590 ± 1.161	0.048
	Rv0563	<i>htpX</i>	0.915 ± 0.027	1.987 ± 0.151	0.037
	Rv0350	<i>dnaK</i>	1.068 ± 0.020	4.734 ± 0.078	0.006
Virulence/detoxification	Rv0170	<i>mce1B</i>	1.055 ± 0.015	2.300 ± 0.233	0.039
	Rv0172	<i>mce1D</i>	1.023 ± 0.009	1.856 ± 0.164	0.050
	Rv0174	<i>mce1F</i>	1.005 ± 0.013	2.368 ± 0.168	0.025
	Rv3757c	<i>proW</i>	0.946 ± 0.021	1.814 ± 0.022	0.0002
	Rv3891c	<i>esxD</i>	0.907 ± 0.011	2.208 ± 0.311	0.050
	Rv3890c	<i>esxC</i>	1.045 ± 0.010	1.976 ± 0.071	0.014
	Rv3913	<i>trxB2</i>	0.979 ± 0.018	5.060 ± 0.319	0.005
	Rv2094c	<i>tatA</i>	0.979 ± 0.018	1.750 ± 0.100	0.020
Transcription	Rv0182c	<i>sigG</i>	1.066 ± 0.018	1.674 ± 0.018	0.003
	Rv3286c	<i>sigF</i>	0.287 ± 0.002	1.963 ± 0.194	0.025
	Rv1221	<i>sigE</i>	0.875 ± 0.0004	2.944 ± 0.317	0.034
	Rv3223c	<i>sigH</i>	0.869 ± 0.029	2.745 ± 0.371	0.047
	Rv2711	<i>ideR</i>	1.026 ± 0.007	1.957 ± 0.186	0.046
	Rv1963c	<i>mce3R</i>	1.078 ± 0.004	2.148 ± 0.057	0.011
	Rv3295		1.017 ± 0.037	1.887 ± 0.002	0.009
	Rv2745c		1.015 ± 0.061	3.903 ± 0.496	0.033
	Rv2884		0.659 ± 0.059	2.237 ± 0.407	0.048
	Rv1674c		1.056 ± 0.125	3.504 ± 0.412	0.048
Transport	Rv2397c	<i>cysA1</i>	0.944 ± 0.006	6.604 ± 1.143	0.0005
	Rv2399c	<i>cysT</i>	0.831 ± 0.035	4.595 ± 0.462	0.003
	Rv2398c	<i>cysW</i>	1.110 ± 0.012	3.995 ± 0.408	0.031
	Rv0655	<i>mkl</i>	1.092 ± 0.029	1.935 ± 0.036	0.038
	Rv1992c	<i>ctpG</i>	0.916 ± 0.060	3.354 ± 0.134	0.001
	Rv3270	<i>ctpC</i>	1.081 ± 0.022	2.987 ± 0.400	0.049
	Rv2400c	<i>subI</i>	1.386 ± 0.028	5.680 ± 0.459	0.022
Sulfate metabolism	Rv0848	<i>cysK2</i>	0.842 ± 0.072	2.452 ± 0.395	0.044
	Rv1336	<i>cysM</i>	0.914 ± 0.058	7.884 ± 1.464	0.044
Cell wall associated	Rv1338	<i>murI</i>	0.746 ± 0.050	2.777 ± 0.393	0.048
	Rv0847	<i>lpqS</i>	1.066 ± 0.088	5.469 ± 0.135	0.002
	Rv2349c	<i>plcC</i>	0.991 ± 0.011	1.726 ± 0.180	0.050
	Rv2051c	<i>ppm1</i>	1.370 ± 0.181	1.827 ± 0.274	0.045
	MT0056	<i>ponA</i>	0.988 ± 0.013	1.722 ± 0.172	0.047
Protein turnover	Rv0782	<i>ptrBb</i>	1.122 ± 0.008	1.770 ± 0.296	0.009
	Rv2110c	<i>prcB</i>	0.814 ± 0.034	1.624 ± 0.087	0.036
	Rv0983	<i>pepD</i>	1.080 ± 0.026	1.692 ± 0.416	0.029
	Rv3596c	<i>clpC1</i>	1.077 ± 0.015	2.553 ± 0.137	0.009
	Rv2461c	<i>clpP1</i>	1.118 ± 0.011	2.258 ± 0.010	0.004
	Rv2460c	<i>clpP2</i>	1.103 ± 0.014	2.835 ± 0.125	0.018
	Rv2457c	<i>clpX</i>	1.306 ± 0.016	1.901 ± 0.140	0.046
Energy metabolism	Rv3053c	<i>nrhH</i>	1.126 ± 0.003	1.896 ± 0.170	0.046
	Rv3146	<i>nuoB</i>	0.917 ± 0.013	1.998 ± 0.170	0.032
	Rv3147	<i>nuoC</i>	0.673 ± 0.012	2.095 ± 0.286	0.046
	Rv3150	<i>nuoF</i>	1.015 ± 0.031	2.011 ± 0.260	0.050
	Rv3153	<i>nuoI</i>	1.008 ± 0.021	2.410 ± 0.330	0.048
	Rv3154	<i>nuoJ</i>	0.920 ± 0.00008	1.881 ± 0.212	0.049
	Rv3155	<i>nuoK</i>	0.916 ± 0.005	1.860 ± 0.223	0.039
	Rv3158	<i>nuoN</i>	0.848 ± 0.013	1.667 ± 0.155	0.045

<sup>a</sup> The functional categorization of *M. tuberculosis* genes was based on their known functions as assigned by the TubercuList database (<http://genolist.pasteur.fr/TubercuList/>). For each gene, the changes in wild-type *M. tuberculosis* relative to the levels for the  $\Delta\text{-}\sigma^H$  mutant in the pre-diamide stress samples and the 60-min-PDS samples are shown, along with standard deviations. Statistical significance was assigned using the ANOVA function within the S<sup>+</sup> ArrayAnalyzer script.



TABLE 6. Genes repressed in wild-type *M. tuberculosis*, relative to the levels for the  $\Delta\text{-}\sigma^H$  mutant, at 60 min PDS<sup>a</sup>

Function	Locus tag	Gene	Fold expression		P	
			Pre-diamide stress	60 min PDS		
Lipid metabolism	Rv0973c	<i>accA2</i>	1.203 ± 0.105	0.488 ± 0.023	0.040	
	Rv2247	<i>accD6</i>	0.840 ± 0.009	0.600 ± 0.027	0.035	
	Rv3252c	<i>alkB</i>	1.427 ± 0.029	0.250 ± 0.025	0.010	
	Rv1094	<i>desA2</i>	0.655 ± 0.006	0.394 ± 0.062	0.048	
	Rv1185c	<i>fadD21</i>	1.061 ± 0.057	0.504 ± 0.051	0.002	
	Rv3089	<i>fadD13</i>	0.965 ± 0.002	0.220 ± 0.053	0.009	
	Rv0404	<i>fadD30</i>	1.135 ± 0.045	0.555 ± 0.037	0.002	
	Rv2950c	<i>fadD29</i>	1.051 ± 0.003	0.396 ± 0.033	0.012	
	Rv2930	<i>fadD26</i>	1.066 ± 0.022	0.121 ± 0.043	0.012	
	Rv1483	<i>fabG1</i>	1.788 ± 0.025	0.421 ± 0.133	0.017	
	Rv2524c	<i>fas</i>	0.870 ± 0.047	0.419 ± 0.055	0.050	
	Rv2384	<i>mbtA</i>	1.097 ± 0.080	0.545 ± 0.074	0.002	
	Rv2382c	<i>mbtC</i>	0.681 ± 0.043	0.424 ± 0.007	0.042	
	Rv2381c	<i>mbtD</i>	0.801 ± 0.040	0.375 ± 0.054	0.050	
	Rv2379c	<i>mbtF</i>	0.854 ± 0.003	0.488 ± 0.064	0.037	
	Rv2931	<i>ppsA</i>	0.991 ± 0.016	0.256 ± 0.100	0.036	
	Rv2932	<i>ppsB</i>	0.808 ± 0.067	0.407 ± 0.059	0.004	
	Rv2933	<i>ppsC</i>	1.293 ± 0.033	0.337 ± 0.072	0.024	
	Rv2934	<i>ppsD</i>	1.303 ± 0.107	0.527 ± 0.205	0.029	
	Rv2935	<i>ppsE</i>	0.852 ± 0.001	0.498 ± 0.076	0.047	
	Rv0405	<i>pks6</i>	1.068 ± 0.020	0.390 ± 0.010	0.007	
	Information pathways	Rv0651	<i>rplJ</i>	1.022 ± 0.037	0.566 ± 0.095	0.028
		Rv2442c	<i>rplU</i>	1.051 ± 0.023	0.589 ± 0.022	0.022
Rv1015c		<i>rplY</i>	0.875 ± 0.008	0.531 ± 0.008	0.011	
Rv2057c		<i>rpmG1</i>	1.032 ± 0.085	0.609 ± 0.016	0.036	
Rv0718		<i>rpsH</i>	1.117 ± 0.121	0.500 ± 0.006	0.041	
Rv2055c		<i>rpsR2</i>	0.814 ± 0.013	0.552 ± 0.013	0.017	
Rv0710		<i>rpsQ</i>	1.115 ± 0.030	0.609 ± 0.003	0.013	
Transport	Rv0917	<i>betP</i>	0.890 ± 0.022	0.541 ± 0.083	0.039	
	Rv2937	<i>drrB</i>	0.781 ± 0.019	0.496 ± 0.002	0.017	
	Rv2938	<i>drrC</i>	1.059 ± 0.019	0.527 ± 0.028	0.054	
	Rv2846c	<i>efpA</i>	0.906 ± 0.085	0.417 ± 0.085	0.0001	
	Rv1811	<i>mgcC</i>	0.941 ± 0.031	0.635 ± 0.008	0.016	
	Rv2281	<i>pitB</i>	1.112 ± 0.001	0.490 ± 0.057	0.020	
	MT0955	<i>pstS1</i>	1.693 ± 0.007	0.596 ± 0.029	0.007	
	Rv1217c		1.120 ± 0.009	0.608 ± 0.064	0.032	
	Rv0986		0.789 ± 0.034	0.452 ± 0.109	0.050	
	Rv0987		0.996 ± 0.052	0.477 ± 0.049	0.044	
	Rv1349		0.904 ± 0.014	0.566 ± 0.060	0.050	

<sup>a</sup> The functional categorization of *M. tuberculosis* genes was based on their known functions as assigned by the TubercuList database (<http://genolist.pasteur.fr/TubercuList/>). For each gene, the changes in wild-type *M. tuberculosis* relative to the levels for the  $\Delta\text{-}\sigma^H$  mutant in the pre-diamide stress samples and the 60-min-PDS samples are shown, along with standard deviations. Statistical significance was assigned using the ANOVA function within the S<sup>+</sup> ArrayAnalyzer script.

demonstrates the temporal plasticity of gene expression in *M. tuberculosis* in response to stress. The pathogen is able to effectively silence expensive, energy-consuming cellular processes, like fatty acid biosynthesis, immediately following oxidative stress, under conditions where lipids can also be oxidized and permanently damaged. With the passage of time, the deleterious effects of oxidative stress are nullified and *M. tuberculosis* resumes fatty acid biosynthesis.

Our results show that  $\sigma^H$  induces the expression of a large number of *M. tuberculosis* transcriptional regulators. This in turn reshapes global transcription in *M. tuberculosis*, silencing lipid and virulence factor biosynthesis until the stress has been effectively managed, while inducing the expression of key regulons involved in virulence, detoxification, and protein processing. Here, we focus our attention on a few key transcription networks controlled by  $\sigma^H$ .

#### The ATP-dependent Clp proteolysis regulon is upregulated

**PDS.** Clp proteases perform regulatory functions by controlling the availability of key enzymes or regulators (18). The *M. tuberculosis* genome encodes two proteolytic (*clpP1* and *clpP2*) and three catalytic (*clpC1*, *clpC2*, and *clpX*) Clp complex subunits (10, 13). In *Corynebacterium glutamicum* and *Streptomyces coelicolor*, expression of the *clp* operon is regulated by a transcription factor, ClgR (*clp* gene regulator), a homolog of Rv2745c (4, 12). The expression of the Rv2745c gene was induced beginning at 30 min PDS (Fig. 6A). The expressions of *clpP1*, *clpP2*, *clpC1* (but not *clpC2*), *clpX*, and *clpS* were also induced at 30 min PDS and peaked at the 60-min-PDS time point. When the *M. tuberculosis* CDC1551 MT2816 gene (Rv2745c) was conditionally induced, the expression levels of the *clp* regulon genes *clpP1*, *clpP2*, and *clpC1* were highly upregulated (Fig. 4). We conclude that the Rv2745c gene

TABLE 7. Genes induced in wild-type *M. tuberculosis*, relative to the levels for the  $\Delta\text{-}\sigma^{\text{H}}$  mutant, at 90 min PDS<sup>a</sup>

Function	Locus tag	Gene	Fold expression		P
			Pre-diamide stress	90 min PDS	
Lipid metabolism	Rv3667	<i>acs</i>	0.921 ± 0.057	1.722 ± 0.154	0.050
	Rv0468	<i>fadB2</i>	1.355 ± 0.033	2.628 ± 0.040	0.007
	Rv1185c	<i>fadD21</i>	1.106 ± 0.057	2.284 ± 0.167	0.042
	Rv0231	<i>fadE4</i>	1.166 ± 0.016	1.755 ± 0.087	0.026
	Rv0242c	<i>fabG4</i>	1.091 ± 0.023	2.196 ± 0.076	0.010
	Rv1493	<i>mutB</i>	1.106 ± 0.016	1.727 ± 0.172	0.055
	Rv1182	<i>papA3</i>	1.265 ± 0.091	2.071 ± 0.148	0.052
	Rv2946c	<i>pks1</i>	0.850 ± 0.038	1.660 ± 0.225	0.051
	Rv2935	<i>ppeE</i>	0.852 ± 0.001	1.791 ± 0.153	0.036
Transport	Rv2920c	<i>amt</i>	1.029 ± 0.053	1.667 ± 0.197	0.049
	Rv2397c	<i>cysA1</i>	0.944 ± 0.006	2.194 ± 0.056	0.011
	Rv3117	<i>cysA3</i>	1.141 ± 0.014	1.702 ± 0.051	0.014
	Rv2398c	<i>cysW</i>	1.110 ± 0.012	1.778 ± 0.043	0.010
	Rv0908	<i>ctpE</i>	1.030 ± 0.033	1.978 ± 0.262	0.051
	Rv1811	<i>mgtC</i>	0.941 ± 0.031	1.564 ± 0.153	0.001
	Rv2281	<i>pitB</i>	1.112 ± 0.001	2.018 ± 0.211	0.046
	Rv1273c		0.872 ± 0.034	3.093 ± 0.576	0.055
	Rv1458c		1.119 ± 0.024	2.166 ± 0.150	0.027
Cell wall associated	Rv3793	<i>embC</i>	0.953 ± 0.004	1.982 ± 0.211	0.046
	Rv0399c	<i>lpqK</i>	0.974 ± 0.113	4.103 ± 0.553	0.047
	Rv1235	<i>lpqY</i>	1.080 ± 0.035	2.113 ± 0.014	0.004
	Rv1921c	<i>lppF</i>	1.244 ± 0.266	3.160 ± 0.567	0.035
	Rv2945c	<i>lppX</i>	0.783 ± 0.029	2.214 ± 0.272	0.045
	Rv0451c	<i>mmpS4</i>	0.893 ± 0.013	2.082 ± 0.165	0.033
	Rv2350c	<i>plcB</i>	0.974 ± 0.010	2.247 ± 0.272	0.045
	Rv3682	<i>ponA2</i>	1.135 ± 0.019	1.771 ± 0.152	0.046
	Rv0284		0.846 ± 0.015	2.213 ± 0.370	0.050
Rv1184c		1.486 ± 0.037	3.460 ± 0.010	0.003	
PE/PPE family	Rv2768c	<i>PPE43</i>	0.878 ± 0.049	1.850 ± 0.082	0.030
	Rv3478	<i>PPE60</i>	1.150 ± 0.024	1.652 ± 0.140	0.050
	Rv1172c	<i>PE12</i>	0.910 ± 0.0003	1.720 ± 0.174	0.047
	Rv1787	<i>PPE25</i>	1.128 ± 0.003	2.219 ± 0.230	0.047
	Rv2519	<i>PE26</i>	1.047 ± 0.052	1.643 ± 0.189	0.050
	Rv1789	<i>PPE26</i>	0.871 ± 0.037	1.680 ± 0.144	0.049
	Rv1430	<i>PE16</i>	1.013 ± 0.046	1.746 ± 0.209	0.049
	Rv3533c	<i>PPE62</i>	1.117 ± 0.033	2.557 ± 0.390	0.050
			0.890 ± 0.022	0.541 ± 0.083	0.039
Protein processing	Rv3596c	<i>clpC1</i>	1.077 ± 0.015	1.651 ± 0.026	0.016
	Rv2460c	<i>clpP2</i>	1.103 ± 0.014	1.838 ± 0.191	0.051
	Rv2461c	<i>clpP1</i>	1.118 ± 0.011	1.624 ± 0.049	0.016
Transcription	Rv3132c	<i>devS</i>	1.037 ± 0.069	2.556 ± 0.432	0.050
	Rv1479	<i>moxR1</i>	0.875 ± 0.0008	1.965 ± 0.013	0.003
	Rv2088	<i>pknJ</i>	0.984 ± 0.159	1.771 ± 0.326	0.047
	Rv1032c	<i>trcS</i>	1.012 ± 0.080	1.949 ± 0.137	0.044

<sup>a</sup> The functional categorization of *M. tuberculosis* genes was based on their known functions as assigned by the TubercuList database (<http://genolist.pasteur.fr/TubercuList/>). For each gene, the changes in wild-type *M. tuberculosis* relative to the levels for the  $\Delta\text{-}\sigma^{\text{H}}$  mutant in the pre-diamide stress samples and the 90-min-PDS samples are shown, along with standard deviations. Statistical significance was assigned using the ANOVA function within the S<sup>+</sup> ArrayAnalyzer script.

product positively regulates the expression of the *M. tuberculosis* ATP-dependent *clp* proteolysis regulon. The expression of Rv2745c is dependent on  $\sigma^{\text{E}}$  (14, 51), which is itself induced in a  $\sigma^{\text{H}}$ -dependent manner upon diamide stress (25, 30) as well as in a  $\sigma^{\text{H}}$ -dependent manner under yet other stress conditions (21). At this time, we are not certain if  $\sigma^{\text{H}}$  indirectly induces Rv2745c expression via  $\sigma^{\text{E}}$  or if it can also directly initiate transcription from the Rv2745c promoter. The promoter sequences recognized by *M. tuberculosis*  $\sigma^{\text{H}}$  and  $\sigma^{\text{E}}$  are remarkably similar, with the exception of the 3' position of the -35 element (51). It is conceivable that the expression of Rv2745c

is induced by  $\sigma^{\text{E}}$  under certain conditions where  $\sigma^{\text{H}}$  is not induced, e.g., upon cell wall damage by SDS (28), or under conditions where neither  $\sigma^{\text{H}}$  nor  $\sigma^{\text{E}}$  is induced, e.g., upon treatment with thioridazine (N. K. Dutta, S. Mehra, and D. Kaushal, submitted for publication), and by both  $\sigma^{\text{H}}$  and  $\sigma^{\text{E}}$  during oxidative and heat stress.

**Regulation of sulfate transport following PDS.** Sulfate assimilation is crucial for *M. tuberculosis*. It is an essential bio-nutrient with a key role in biosynthesis of cysteine, mycothiol, and coenzyme A. Moreover, extracellular presentation of sulfated metabolites may regulate host-pathogen and cell-cell

TABLE 8. Genes repressed in wild-type *M. tuberculosis*, relative to the levels for the  $\Delta\text{-}\sigma^H$  mutant, at 90 min PDS<sup>a</sup>

Function	Locus tag	Gene	Fold expression		P
			Pre-diamide stress	90 min PDS	
Virulence	Rv3667	<i>hbhA</i>	1.203 ± 0.010	0.502 ± 0.185	0.051
Lipid metabolism	Rv3825c	<i>pks2</i>	2.535 ± 0.003	0.550 ± 0.320	0.037
Hypothetical proteins	MT1775		1.283 ± 0.003	0.339 ± 0.117	0.031

<sup>a</sup> The functional categorization of *M. tuberculosis* genes was based on their known functions as assigned by the TubercuList database (<http://genolist.pasteur.fr/TubercuList/>). For each gene, the changes in wild-type *M. tuberculosis* relative to the levels for the  $\Delta\text{-}\sigma^H$  mutant in the pre-diamide stress samples and the 90-min-PDS samples are shown, along with standard deviations. Statistical significance was assigned using the ANOVA function within the S<sup>+</sup> ArrayAnalyzer script.

communication (6). The CysTWA SubI ABC transporter complex is responsible for the active transport of inorganic sulfate across the mycobacterial cell membrane. Once imported, sulfate is phosphorylated to adenosine-5-phosphosulfate (APS) and then to 3'-phosphoadenosine 5'-phosphosulfate (PAPS), a universal sulfate donor, in a two-step reaction catalyzed by the bifunctional enzyme encoded by *cysNC*. GTP hydrolysis performed by the *cysD* product provides energy for this energetically unfavorable reaction. Together, the *cysNC*- and *cysD*-encoded proteins form a sulfate-activating complex. The sulfate moiety in APS can be reduced to sulfite by the *cysH* product in a reaction catalyzed by thioredoxin. Sulfite can be further reduced to sulfide by the *nirA*-encoded sulfite reductase (ferredoxin-dependent nitrite reductase). Sulfide is used to biosynthesize cysteine, methionine, coenzyme A, and mycothiol. De novo synthesis of cysteine involves the generation of *O*-acetyl-L-serine either by the *cysE* product, in which case it is condensed with a reduced sulfide by-product of *cysK2* or *cysM*, or by the *cysO* and *moeZ* gene products. The expressions of *cysD* and *cysNC* were induced in wild-type *M. tuberculosis*, relative to the level for  $\Delta\text{-}\sigma^H$ , at 30 min PDS. These genes have also been induced during stationary-phase growth (19) and upon reactive nitrogen (36) or oxidative (40) stress. The expressions of *cysH* and *nirA* (Rv2391) were induced at 90 and 120 min PDS in *M. tuberculosis*, although the level of *cysH* induction was below the stringent statistical-significance levels employed by us. The *cysE*, *cysM*, *cysO*, and *moeZ* genes were also induced in *M. tuberculosis* following stress. These results show that an entire network of genes involved in sulfate acquisition from the environment and its reduction to biologi-

cally utilizable forms for biosynthetic processes was activated. This underscores the crucial role of sulfate metabolism in the constitution of mycobacterial proteins, enzymes, and other biologically active compounds.

**Regulation of the *mce1* operon.** The *mce1* operon is important for the virulence of *M. tuberculosis* (49). The six Mce1 proteins (Mce1A to Mce1F) interact with host components during infection and influence the immune response. The *M. tuberculosis mce1* mutants have aberrant inflammatory cell migration and poor granuloma formation, resulting in uncontrolled bacterial growth and rapid death of mutant-infected mice (49). Members of the *mce1* operon have been shown to be coexpressed with  $\sigma^H$  and  $\sigma^E$  upon phagocytosis by human macrophages (19). In this report, we show that the expressions of several members of the *mce1* regulon are induced as a result of oxidative stress. These include *mce1A*, *mce1C*, and *mce1E* (30 min) and *mce1B* and *mce1D* (30 and 60 min). While we do not know the identity of the factor that directly mediates the expression of the *mce1* regulon following oxidative stress, it is likely that  $\sigma^H$  is not directly involved. The induction of  $\sigma^H$  following oxidative stress perhaps serves as a cue for the pathogen to induce its key virulence functions in order to disseminate to secondary cells.

**Transcriptional networks in *M. tuberculosis* following  $\sigma^H$  induction.** Modulation of the gene expression of numerous transcription factors helps  $\sigma^H$  mediate its long-term impact. The function of the Rv2745c-encoded transcription factor has already been discussed. Other transcription factors whose expression levels were perturbed in wild-type *M. tuberculosis* relative to the level for the mutant include Rv0273c, Rv0324,

TABLE 9. Genes induced in wild-type *M. tuberculosis*, relative to the levels for the  $\Delta\text{-}\sigma^H$  mutant, at 120 min PDS<sup>a</sup>

Function	Locus tag	Gene	Fold expression		P
			Pre-diamide stress	120 min PDS	
Transport	Rv1183	<i>mmpL10</i>	0.911 ± 0.221	1.666 ± 0.074	0.044
	Rv0929	<i>pstC2</i>	1.086 ± 0.034	1.756 ± 0.059	0.031
	Rv2281	<i>pitB</i>	1.112 ± 0.001	1.883 ± 0.164	0.047
	Rv2397c	<i>cysA1</i>	0.944 ± 0.006	1.610 ± 0.148	0.050
Intermediary metabolism	Rv1318c	<i>adc</i>	1.130 ± 0.295	1.996 ± 0.384	0.023
	Rv3303c	<i>lpdA</i>	1.309 ± 0.026	1.809 ± 0.032	0.034
	Rv0557	<i>pimB</i>	1.385 ± 0.021	3.026 ± 0.348	0.044
	Rv0886	<i>fprB</i>	1.022 ± 0.077	1.841 ± 0.113	0.051
	Rv0373c	<i>coxM</i>	1.336 ± 0.029	3.246 ± 0.336	0.042

<sup>a</sup> The functional categorization of *M. tuberculosis* genes was based on their known functions as assigned by the TubercuList database (<http://genolist.pasteur.fr/TubercuList/>). For each gene, the changes in wild-type *M. tuberculosis* relative to the levels for the  $\Delta\text{-}\sigma^H$  mutant in the pre-diamide stress samples and the 120-min-PDS samples are shown, along with standard deviations. Statistical significance was assigned using the ANOVA function within the S<sup>+</sup> ArrayAnalyzer script.

TABLE 10. Genes repressed in wild-type *M. tuberculosis*, relative to the levels for the  $\Delta\sigma^H$  mutant, at 120 min PDS<sup>a</sup>

Function	Locus tag	Gene	Fold expression		<i>P</i>
			Pre-diamide stress	120 min PDS	
Heat shock	Rv3418c	<i>groES</i>	1.342 ± 0.003	0.580 ± 0.023	0.007
	Rv0440	<i>groEL2</i>	1.075 ± 0.0003	0.580 ± 0.0003	0.010
	Rv0251c	<i>hsp</i>	0.951 ± 0.048	0.613 ± 0.050	0.032
Virulence	Rv3875	<i>esxA</i>	1.083 ± 0.0005	0.590 ± 0.037	0.017
	Rv3874	<i>esxB</i>	0.993 ± 0.035	0.580 ± 0.023	0.006
	Rv0287	<i>esxG</i>	0.941 ± 0.018	0.580 ± 0.023	0.003
	Rv0288	<i>esxH</i>	1.176 ± 0.021	0.580 ± 0.021	0.016
	Rv1793	<i>esxN</i>	1.068 ± 0.036	0.570 ± 0.009	0.020
	Rv3019c	<i>esxR</i>	1.215 ± 0.018	0.586 ± 0.032	0.004
	Molybdenum biosynthesis	MT3193	<i>moaB1</i>	1.798 ± 0.118	0.539 ± 0.111
	Rv3111	<i>moaC1</i>	ND	0.622 ± 0.026	0.093
	Rv3112	<i>moaD1</i>	ND	0.345 ± 0.067	0.023
	Rv0868c	<i>moaD2</i>	1.233 ± 0.024	0.565 ± 0.082	0.019

<sup>a</sup> The functional categorization of *M. tuberculosis* genes was based on their known functions as assigned by the TubercuList database (<http://genolist.pasteur.fr/TubercuList/>). For each gene, the changes in wild-type *M. tuberculosis* relative to the levels for the  $\Delta\sigma^H$  mutant in the pre-diamide stress samples and the 120-min-PDS samples are shown, along with standard deviations. Statistical significance was assigned using the ANOVA function within the S<sup>+</sup> ArrayAnalyzer script. ND, not determined.

Rv0348, Rv0465c, Rv1019, Rv1049, Rv1129c, Rv1674c, Rv1956, Rv3291c, and Rv3692. Rv3291c encodes LrpA, a feast/famine family member that is induced during anaerobic conditions (55) and nutritional starvation (5) and is critical for

persistence (39). Its *Escherichia coli* homolog regulates metabolic pathways in response to the availability of amino acids in the external environment (8). While we do not know which *M. tuberculosis* genes are regulated by *lrpA*, a large number of

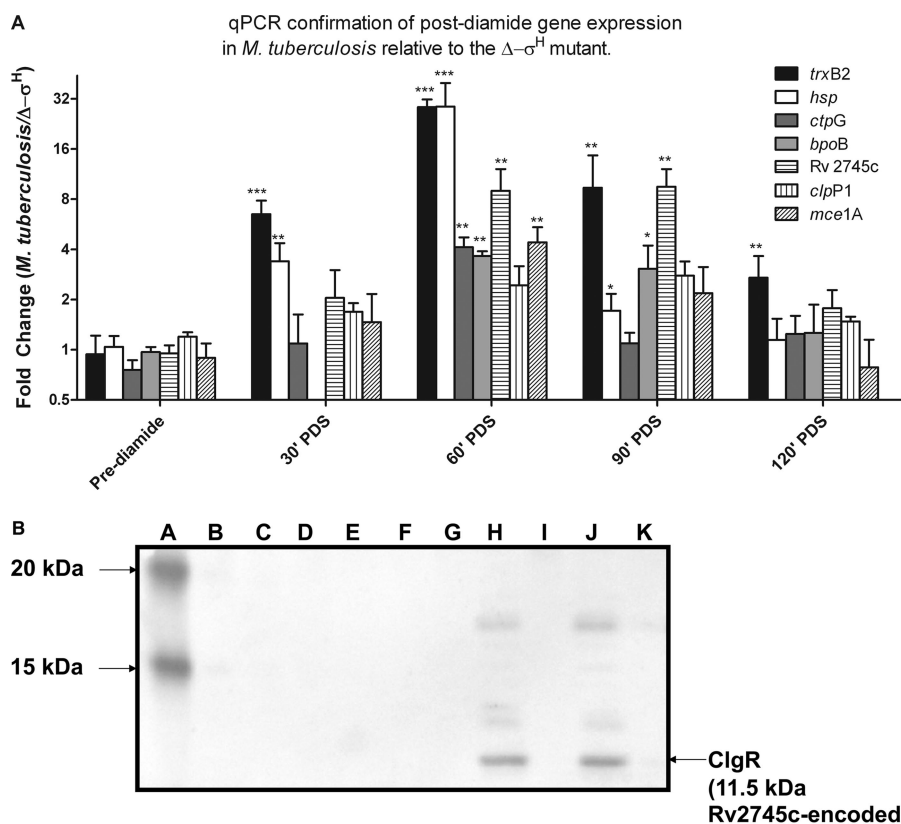


FIG. 3. Confirmation of the PDS microarray data. (A) qPCR-based interrogation of the PDS expression levels of certain genes with perturbed expression in wild-type *M. tuberculosis* relative to the level for the  $\Delta\sigma^H$  mutant at different time points. Results are shown for *trxB2*, *hsp*, *ctpG*, *bpoB*, Rv2745c, *clpP1*, and *mce1A*. Values represent mean differences (*n*-fold) ± standard deviations of results from quadruplicate experiments. Statistically significant changes in expression are denoted by \* ( $P < 0.05$ ), \*\* ( $P < 0.01$ ), or \*\*\* ( $P < 0.005$ ). (B) Western blot of *M. tuberculosis* wild-type and  $\Delta\sigma^H$  mutant lysates obtained from cultures treated pre-diamide stress and PDS shows a  $\sigma^H$ -dependent expression of Rv2745c. Lysates were probed with an affinity-purified polyclonal antibody raised against an epitope on the protein encoded by the *M. tuberculosis* Rv2745c gene. Lane A, prestained protein ladder (Invitrogen); lane B, lysate from log-phase pre-diamide stress *M. tuberculosis* culture; lane C, lysate from log-phase pre-diamide stress  $\Delta\sigma^H$  culture; lanes D, F, H, and J, lysates from 0-, 30-, 60-, and 90-min-PDS *M. tuberculosis* cultures; lanes E, G, I, and K, lysates from 0-, 30-, 60-, and 90-min-PDS  $\Delta\sigma^H$  cultures.

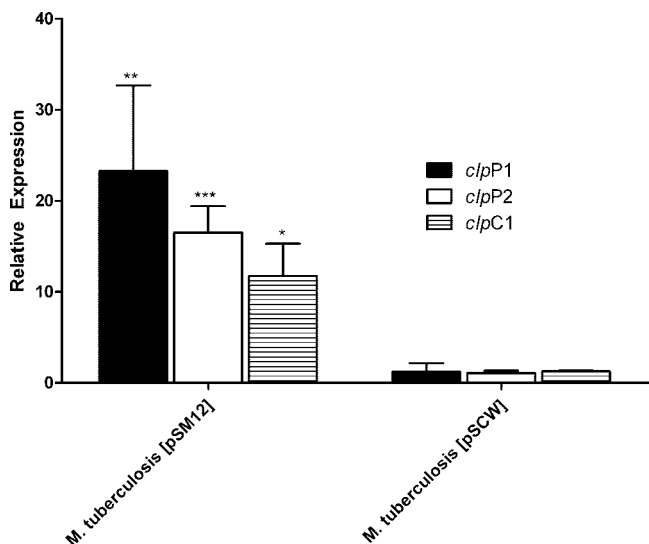


FIG. 4. qPCR-based analysis of the expression of *clp* regulon genes following acetamide-dependent induction of the Rv2745c gene in *M. tuberculosis*. qPCR was used to interrogate the expression levels of *clpP1*, *clpP2*, and *clpC1* following induction of the Rv2745c gene. Results are shown for *M. tuberculosis*(pSM12) (carrying an integrative vector with Rv2745c in a transcriptional fusion with the *M. smegmatis* acetamidase promoter) and *M. tuberculosis*(pSCW38) (carrying an integration-proficient vector with the acetamidase promoter without any gene, as a control). Values represent mean differences (*n*-fold)  $\pm$  standard deviations of results from quadruplicate experiments. Statistically significant changes in expression are denoted by \* ( $P < 0.05$ ), \*\* ( $P < 0.01$ ), or \*\*\* ( $P < 0.005$ ).

genes related to amino acid metabolism were induced at 60 min PDS, following the induction of *hpaA* at 30 min PDS.

The Rv0324-Rv0325-Rv0326 operon is induced in enduring hypoxia, along with the  $\sigma^H/\sigma^E$  regulon (48). The Rv0347-

Rv0348-Rv0349 operon is induced in vivo at the late stage of chronic TB (53). Rv0348 potentiates the expression of  $\sigma^F$ , which orchestrates entry into the chronic stage of TB (15). The expression of Rv1049 is induced by heat shock (52), peroxide stress (48), and starvation (5). Rv1049 is required for survival in murine macrophages (43). Rv1956 is induced by starvation (5) and encodes a possible antitoxin. Rv0465c is induced following nutritional stress (20) in a  $\sigma^E$ - and  $\sigma^F$ -dependent manner. The expressions of Rv1129c and its adjoining genes Rv1130 and Rv1131 are induced in a  $\sigma^E$  (29)- and *mprA*-dependent manner (37).

The Rv1994c (*cmtR*)-encoded repressor CmtR senses the critical thresholds of Cd(II) and Pb(II) (9), is induced during starvation (5) and oxidative stress (48), and is required for in vivo survival (24). We propose that diamide treatment oxidizes the numerous cysteine thiols that CmtR senses metal ions through. This derepresses the *cmtR* regulon, leading to the induction of transporters Rv1993 and *ctpG*. This allows *M. tuberculosis* to transport out the high levels of Cd(II) and Pb(II). CmtR is able to sense metal ions upon the restoration of redox homeostasis in *M. tuberculosis*, eventually repressing the Rv1993-*ctpG* operon. We also observed the induction of the *cadI* gene by diamide treatment in *M. tuberculosis*, in contrast to an earlier report (23). However, it must be considered that the earlier report involved the use of the H37Rv strain, not the CDC1551 strain, of *M. tuberculosis*. Alternatively, it is possible that a duration of diamide treatment other than 1 h or a concentration of diamide other than 10 mM was used in the previous report. The function of *M. tuberculosis* CadI appears to be similar to that of metallothioneins, which are low-molecular-weight, cysteine-rich proteins that protect against metal toxicity. Since diamide oxidizes cysteine residues on proteins,

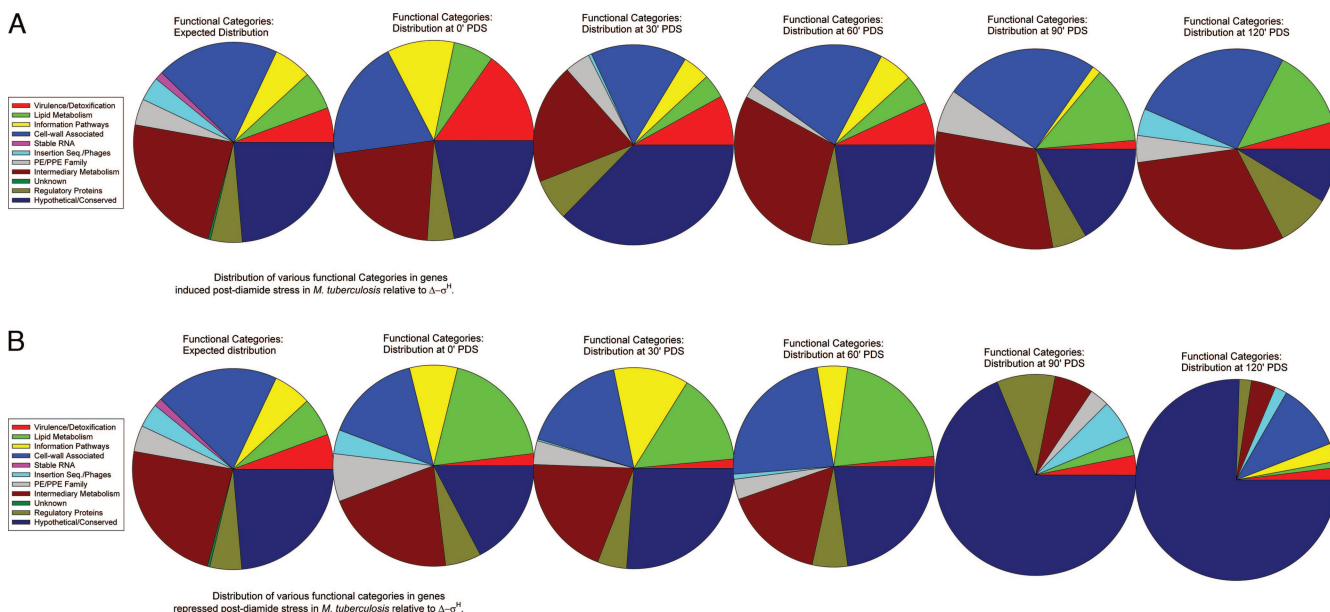


FIG. 5. Functional characterization of the PDS microarray data. Microarray data for each time point (0, 30, 60, 90, and 120 min PDS) were analyzed based on the distribution of various functional categories as defined by the TubercuList database (<http://genolist.pasteur.fr/TubercuList/>) for genes that were induced (A) or repressed (B) in wild-type *M. tuberculosis*, relative to the level for the  $\Delta\sigma^H$  mutant. These results were compared to the expected distribution of different functional categories (pie on the left). The pie sections are arranged in an anticlockwise manner, beginning with a red section for category 0, followed by green and yellow sections for categories 1 and 2, respectively.

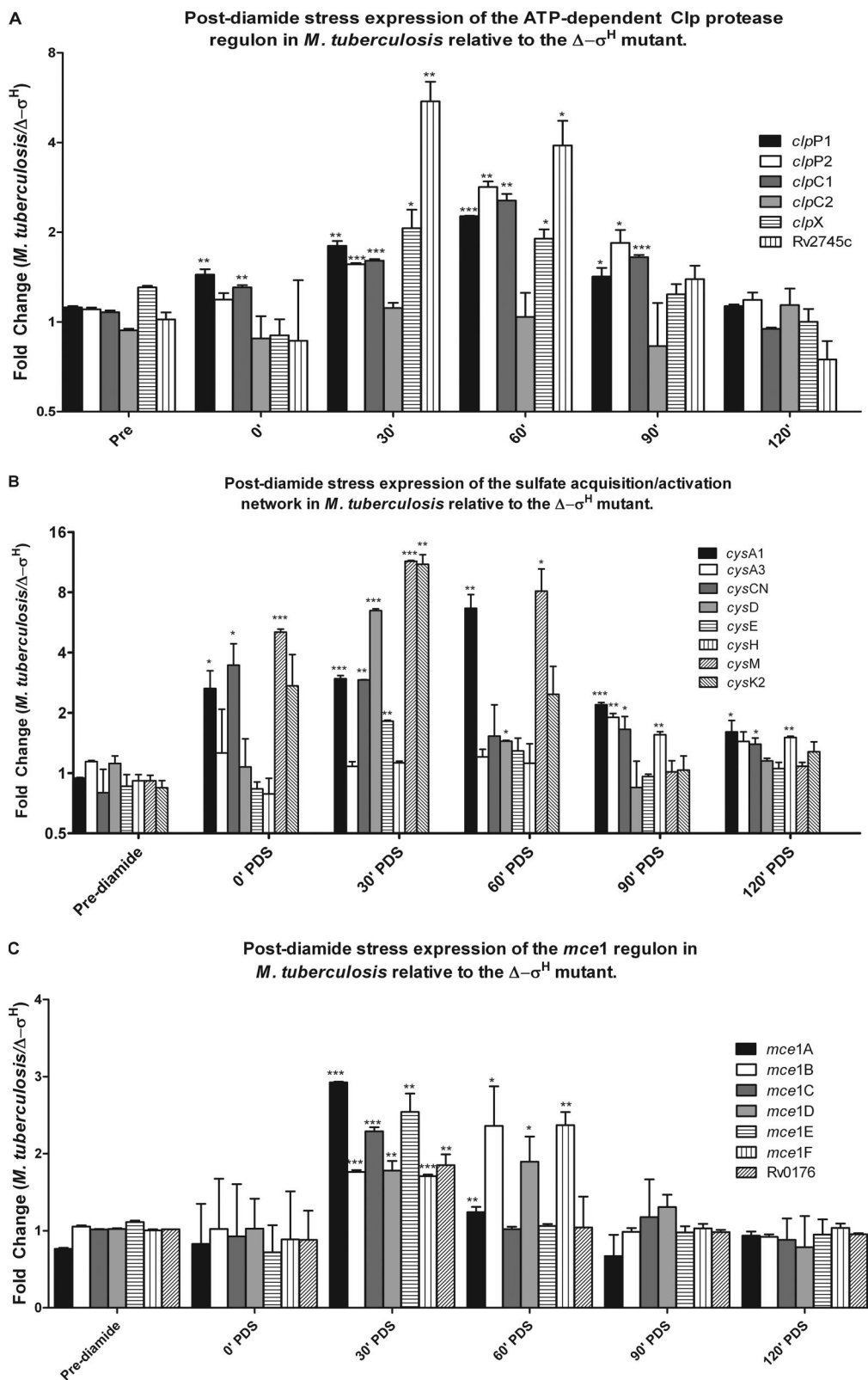


FIG. 6. Genes belonging to the ATP-dependent *clp* regulon, the mammalian cell entry 1 (*mce1*) operon, and the sulfate acquisition/activation network are expressed in a  $\sigma^H$ -dependent manner PDS. The expression levels of *clp* regulon genes *clpP1*, *clpP2*, *clpC1*, *clpC2*, *clpX*, and Rv2745c are presented as means of results from two independent microarray experiments (A). The expression levels of the sulfate transport/activation genes *cysA1*, *cysA3*, *cysCN*, *cysD*, *cysE*, *cysH*, *cysM*, and *cysK2* are presented as means of results from two independent array experiments (B). The expression levels of *mce1* operon genes *mce1A*, *mce1B*, *mce1C*, *mce1D*, *mce1E*, *mce1F*, and Rv0176 are presented as means of results from two independent experiments (C). Statistically significant changes in expression are denoted by \* ( $P < 0.05$ ), \*\* ( $P < 0.01$ ), or \*\*\* ( $P < 0.005$ ).

an increased induction of *cadI* may be an attempt by *M. tuberculosis* to overcome the decreased activity of this protein.

*furA* encodes a global repressor that uses  $Fe^{2+}$  as a cofactor to bind the *katG* operator. *katG* is transcribed from two promoters, one generating a bicistronic *furA-katG* message, expressed initially during infection, and another generating a monocistronic *katG* mRNA, which peaks at a later stage (33). The expression of *furA* was induced at 30 min PDS and then declined. The expression pattern of *katG* was the mirror opposite; this gene was repressed at 30 min PDS, presumably due to repression by *furA*, and then induced as the *furA* levels declined, peaking at 90 min PDS. The iron-binding repressor IdeR reduces the expression of genes involved in siderophore biosynthesis, iron storage, and transport (44), including *mbtABCDEFGHI*, *fadE14*, Rv3402c, and Rv3403c. All these genes exhibited reduced expression in wild-type *M. tuberculosis*, relative to the level for the mutant, at 30 min PDS. The expression of *ideR* is induced by  $\sigma^B$ , which is itself induced in a  $\sigma^H$ -dependent manner following oxidative stress. Rv2358 encodes Zur, which regulates the homeostasis and uptake of zinc, an essential element that is included in numerous enzymes and proteins as a cofactor or a structural scaffold but can be toxic at higher concentrations (28). Rv0981 (*mprA*) encodes a two-component response transcriptional regulatory protein, MprA (mycobacterial persistence regulator), which is induced upon starvation and in a  $\sigma^E$ -dependent manner.

To summarize, we have shown that  $\sigma^H$  not only directs the transcription of a subset of genes involved in the maintenance of redox homeostasis and protein integrity but also induces a network of transcription factors, which further induce crucial bacterial functions, such as ATP-dependent proteolysis of specific targets, acquisition and utilization of environmental sulfate toward the biosynthesis of key mycobacterial metabolites, specific virulence- and pathogenesis-related operons that help *M. tuberculosis* survive and disseminate in vivo, and transcription factors that help *M. tuberculosis* sense and respond to the levels of various metal and trace metal ions. We demonstrate the dynamic nature of the pathogen's response to adverse environmental conditions, with the expression of genes involved in lipid biosynthesis being repressed following oxidative stress and resuming upon the removal of stress. We hope to extend these findings by interrogating their intraphagosomal and in vivo relevance.

#### ACKNOWLEDGMENTS

This work was supported by NIH grants P20RR020159 and P51RR164, with additional support from the Tulane Research Enhancement Fund and the Louisiana Vaccine Center.

We acknowledge excellent technical, secretarial, and graphic design assistance from Sondra LeBreton, Avery MacLean, and Robin Rodriguez, respectively. We are grateful to the PFGRC for DNA microarrays and to Colorado State University for genomic DNA.

#### REFERENCES

- Andersen, P., and T. M. Doherty. 2005. The success and failure of BCG—implications for a novel tuberculosis vaccine. *Nat. Rev. Microbiol.* **3**:656–662.
- Ando, M., T. Yoshimatsu, C. Ko, P. J. Converse, and W. R. Bishai. 2003. Deletion of *Mycobacterium tuberculosis* sigma factor E results in delayed time to death with bacterial persistence in the lungs of aerosol-infected mice. *Infect. Immun.* **71**:7170–7172.
- Arcus, V. L., P. B. Rainey, and S. J. Turner. 2005. The PIN-domain toxin-antitoxin array in mycobacteria. *Trends Microbiol.* **13**:360–365.
- Bellier, A., and P. Mazodier. 2004. ClgR, a novel regulator of *clp* and *lon* expression in *Streptomyces*. *J. Bacteriol.* **186**:3238–3248.
- Betts, J. C., P. T. Lukey, L. C. Robb, R. A. McAdam, and K. Duncan. 2002. Evaluation of a nutrient starvation model of *Mycobacterium tuberculosis* persistence by gene and protein expression profiling. *Mol. Microbiol.* **43**:717–731.
- Bhave, D. P., W. B. Muse III, and K. S. Carroll. 2007. Drug targets in mycobacterial sulfur metabolism. *Infect. Disord. Drug Targets* **7**:140–158.
- Boshoff, H. L., T. G. Myers, B. R. Copp, M. R. McNeil, M. A. Wilson, and C. E. Barry III. 2004. The transcriptional responses of *Mycobacterium tuberculosis* to inhibitors of metabolism: novel insights into drug mechanisms of action. *J. Biol. Chem.* **279**:40174–40184.
- Calvo, J. M., and R. G. Mathews. 1994. Leucine responsive regulatory protein, a global regulator of metabolism in *Escherichia coli*. *Microbiol. Rev.* **58**:466–490.
- Cavet, J. S., A. I. Graham, W. Meng, and N. J. Robinson. 2003. A cadmium-lead-sensing ArsR-SmtB repressor with novel sensory sites. *J. Biol. Chem.* **278**:44560–44566.
- Cole, S. T., R. Brosch, J. Parkhill, T. Garnier, C. Churcher, D. Harris, S. V. Gordon, K. Eiglmeier, S. Gas, C. E. Barry III, F. Tekaiia, K. Badcock, D. Basham, D. Brown, T. Chillingworth, R. Connor, R. Davies, K. Devlin, T. Feltham, S. Gentles, N. Hamlin, S. Holroyd, T. Hornsby, K. Jagels, A. Krogh, J. McLean, S. Moule, L. Murphy, K. Oliver, J. Osborne, M. A. Quail, M. A. Rajandream, J. Rogers, S. Rutter, K. Seeger, J. Skelton, R. Squares, S. Squares, J. E. Sulston, K. Taylor, S. Whitehead, and B. G. Barrell. 1998. Deciphering the biology of *Mycobacterium tuberculosis* from the complete genome sequence. *Nature* **393**:537–544.
- Edwards, K. M., M. H. Cynamon, R. K. Voladri, C. C. Hager, M. S. DeStefano, K. T. Tham, D. L. Lakey, M. R. Bochan, and D. S. Kernodle. 2001. Iron-cofactored superoxide dismutase inhibits host responses to *Mycobacterium tuberculosis*. *Am. J. Respir. Crit. Care Med.* **64**:2213–2219.
- Engels, S., J. E. Schweitzer, C. Ludwig, M. Bott, and S. Schaffer. 2004. *clpC* and *clpP2* gene expression in *Corynebacterium glutamicum* is controlled by a regulatory network involving the transcriptional regulators ClgR and HspR as well as the ECF sigma factor sigmaH. *Mol. Microbiol.* **52**:285–302.
- Fleischmann, R. D., D. Alland, J. A. Eisen, L. Carpenter, O. White, J. Peterson, R. DeBoy, R. Dodson, M. Gwinn, D. Haft, E. Hickey, J. F. Kolonay, W. C. Nelson, L. A. Umayam, M. Ermolaeva, S. L. Salzberg, A. Delcher, T. Utterback, J. Weidman, H. Khouri, J. Gill, A. Mikula, W. Bishai, W. R. Jacobs, Jr., J. C. Venter, and C. M. Fraser. 2002. Whole-genome comparison of *Mycobacterium tuberculosis* clinical and laboratory strains. *J. Bacteriol.* **184**:5479–5490.
- Fontán, P. A., V. Aris, M. E. Alvarez, S. Ghanny, J. Cheng, P. Soteropoulos, A. Trevani, R. Pine, and I. Smith. 2008. *Mycobacterium tuberculosis* sigma factor E regulon modulates the host inflammatory response. *J. Infect. Dis.* **198**:877–885.
- Geiman, D. E., D. Kaushal, C. Ko, S. Tyagi, Y. C. Manabe, B. G. Schroeder, R. D. Fleischmann, N. E. Morrison, P. J. Converse, P. Chen, and W. R. Bishai. 2004. Attenuation of late-stage disease in mice infected by the *Mycobacterium tuberculosis* mutant lacking the SigF alternate sigma factor and identification of SigF-dependent genes by microarray analysis. *Infect. Immun.* **72**:1733–1745.
- Gomez, J. E., J. M. Chen, and W. R. Bishai. 1997. Sigma factors of *Mycobacterium tuberculosis*. *Tuber. Lung Dis.* **78**:175–183.
- Gordhan, B. G., D. A. Smith, H. Alderton, R. A. McAdam, G. J. Bancroft, and V. Mizrahi. 2002. Construction and phenotypic characterization of an auxotrophic mutant of *Mycobacterium tuberculosis* defective in L-arginine biosynthesis. *Infect. Immun.* **70**:3080–3084.
- Gottesman, S. 1996. Proteases and their targets in *Escherichia coli*. *Annu. Rev. Genet.* **30**:465–506.
- Graham, J. E., and J. E. Clark-Curtiss. 1999. Identification of *Mycobacterium tuberculosis* RNAs synthesized in response to phagocytosis by human macrophages by selective capture of transcribed sequences (SCOTS). *Proc. Natl. Acad. Sci. USA* **96**:11554–11559.
- Hampshire, T., S. Soneji, J. Bacon, B. W. James, J. Hinds, R. A. Stabler, P. D. Marsh, and P. D. Butcher. 2004. Stationary phase gene expression of *Mycobacterium tuberculosis* following a progressive nutrient depletion: a model for persistent organisms? *Tuberculosis* **84**:228–238.
- He, H., R. Hovey, J. Kane, V. Singh, and T. C. Zahrt. 2006. MprAB is a stress-responsive two-component system that directly regulates expression of sigma factors SigB and SigE in *Mycobacterium tuberculosis*. *J. Bacteriol.* **188**:2134–2143.
- Hernandez-Abanto, S. M., S. C. Woolwine, S. K. Jain, and W. R. Bishai. 2006. Tetracycline-inducible gene expression in mycobacteria within an animal host using modified *Streptomyces* tcp830 regulatory elements. *Arch. Microbiol.* **186**:459–464.
- Hotter, G. S., T. Wilson, and D. M. Collins. 2001. Identification of a cadmium induced gene in *Mycobacterium bovis* and *Mycobacterium tuberculosis*. *FEMS Microbiol. Lett.* **200**:151–155.
- Jain, S. K., S. M. Hernandez-Abanto, Q.-J. Cheng, P. Singh, L. H. Ly, L. G. Klinkenberg, N. E. Morrison, P. J. Converse, E. Nuermberger, J. Grosset, D. N. McMurray, P. C. Karakousis, G. Lamichhane, and W. R. Bishai. 2007. Accelerated detection of *Mycobacterium tuberculosis* genes essential for bac-

- terial survival in guinea pigs, compared with mice. *J. Infect. Dis.* **195**:1634–1642.
25. Kaushal, D., B. G. Schroeder, S. Tyagi, T. Yoshimatsu, C. Scott, C. Ko, L. Carpenter, J. Mehrotra, Y. C. Manabe, R. D. Fleischmann, and W. R. Bishai. 2002. Reduced immunopathology and mortality despite tissue persistence in a *Mycobacterium tuberculosis* mutant lacking alternative sigma factor, SigH. *Proc. Natl. Acad. Sci. USA* **99**:8330–8335.
  26. Lee, J. H., P. C. Karakousis, and W. R. Bishai. 2008. Roles of SigB and SigF in the *Mycobacterium tuberculosis* sigma factor network. *J. Bacteriol.* **190**:699–707.
  27. Lonetto, M., M. Gribskov, and C. A. Gross. 1992. The sigma 70 family: sequence conservation and evolutionary relationships. *J. Bacteriol.* **174**:3843–3849.
  28. Maciag, A., E. Dainese, G. M. Rodriguez, A. Milano, R. Proveddi, M. R. Pasca, I. Smith, G. Palu, G. Riccardi, and R. Manganelli. 2007. Global analysis of the *Mycobacterium tuberculosis* Zur (FurB) regulon. *J. Bacteriol.* **189**:730–740.
  29. Manganelli, R., M. I. Voskuil, G. K. Schoolnik, and I. Smith. 2001. The *Mycobacterium tuberculosis* ECF sigma factor sigmaE: role in global gene expression and survival in macrophages. *Mol. Microbiol.* **41**:423–437.
  30. Manganelli, R., M. I. Voskuil, G. K. Schoolnik, E. Dubnau, M. Gomez, and I. Smith. 2002. Role of the extracytoplasmic-function sigma factor sigma(H) in *Mycobacterium tuberculosis* global gene expression. *Mol. Microbiol.* **45**:365–374.
  31. Manganelli, R., R. Proveddi, S. Rodrigue, J. Beaucher, L. Gaudreau, and I. Smith. 2004. Sigma factors and global gene regulation in *Mycobacterium tuberculosis*. *J. Bacteriol.* **186**:895–902.
  32. Manganelli, R., L. Fattorini, D. Tan, E. Iona, G. Orefici, G. Altavilla, P. Cusatelli, and I. Smith. 2004. The extra cytoplasmic function sigma factor  $\sigma^E$  is essential for *Mycobacterium tuberculosis* virulence in mice. *Infect. Immun.* **72**:3038–3041.
  33. Master, S., T. C. Zahrt, J. Song, and V. Deretic. 2001. Mapping of *Mycobacterium tuberculosis* *katG* promoters and their differential expression in infected macrophages. *J. Bacteriol.* **183**:4033–4039.
  34. Matteelli, A., G. B. Migliori, D. Cirillo, R. Centis, E. Girard, and M. Raviglione. 2007. Multidrug-resistant and extensively drug-resistant *Mycobacterium tuberculosis*: epidemiology and control. *Expert Rev. Anti Infect. Ther.* **5**:857–871.
  35. Missiakas, D., and S. Raina. 1998. The extracytoplasmic function sigma factors: role and regulation. *Mol. Microbiol.* **28**:1059–1066.
  36. Ohno, H., G. Zhu, V. P. Mohan, D. Chu, S. Kohno, W. R. Jacobs, Jr., and J. Chan. 2003. The effects of reactive nitrogen intermediates on gene expression in *Mycobacterium tuberculosis*. *Cell. Microbiol.* **5**:637–648.
  37. Pang, X., P. Vu, T. F. Byrd, S. Ghanny, P. Soteropoulos, G. V. Mukamolova, S. Wu, B. Samten, and S. T. Howard. 2007. Evidence for complex interactions of stress-associated regulons in a *mprAB* deletion mutant of *Mycobacterium tuberculosis*. *Microbiology* **153**:1229–1242.
  38. Park, S. T., C.-M. Kang, and R. N. Husson. 2008. Regulation of the SigH stress response regulon by an essential protein kinase in *Mycobacterium tuberculosis*. *Proc. Natl. Acad. Sci. USA* **105**:13105–13110.
  39. Parti, R. P., R. Shrivastava, S. Srivastava, A. R. Subramanian, R. Roy, B. S. Srivastava, and R. Srivastava. 2008. A transposon insertion mutant of *Mycobacterium fortuitum* attenuated in virulence and persistence in a murine infection model that is complemented by Rv3291c of *Mycobacterium tuberculosis*. *Microb. Pathog.* **45**:370–376.
  40. Pinto, R., Q. X. Tang, W. J. Britton, T. S., Leyh, and J. A. Triccas. 2004. The *Mycobacterium tuberculosis* *cysD* and *cysNC* genes form a stress-induced operon that encodes a tri-functional sulfate-activating complex. *Microbiology* **150**:1681–1686.
  41. Raman, S., T. Song, X. Puyang, S. Bardarov, W. R. Jacobs, Jr., and R. N. Husson. 2001. The alternative sigma factor SigH regulates major components of oxidative and heat stress responses in *Mycobacterium tuberculosis*. *J. Bacteriol.* **183**:6119–6125.
  42. Raviglione, M. C. 2003. The TB epidemic from 1992 to 2002. *Tuberculosis (Edinburgh)* **83**:4–14.
  43. Rengarajan, J., B. R. Bloom, and E. J. Rubin. 2005. Genome-wide requirements for *Mycobacterium tuberculosis* adaptation and survival in macrophages. *Proc. Natl. Acad. Sci. USA* **102**:8327–8332.
  44. Rodriguez, G. M., M. I. Voskuil, B. Gold, G. K. Schoolnik, and I. Smith. 2002. *ideR*, An essential gene in *Mycobacterium tuberculosis*: role of IdeR in iron-dependent gene expression, iron metabolism, and oxidative stress response. *Infect. Immun.* **70**:3371–3381.
  45. Rohde, K. H., R. B. Abramovitch, and D. G. Russell. 2007. *Mycobacterium tuberculosis* invasion of macrophages: linking bacterial gene expression to environmental cues. *Cell Host Microbe* **2**:352–364.
  46. Rustad, T. R., M. I. Harrell, R. Liao, and D. R. Sherman. 2008. The enduring hypoxic response of *Mycobacterium tuberculosis*. *PLoS ONE* **3**:e1502.
  47. Saint-Joanis, B., C. Demangel, M. Jackson, P. Brodin, L. Marsollier, H. Boshoff, and S. T. Cole. 2006. Inactivation of Rv2525c, a substrate of the twin arginine translocation (Tat) system of *Mycobacterium tuberculosis*, increases  $\beta$ -lactam susceptibility and virulence. *J. Bacteriol.* **188**:6669–6679.
  48. Schnappinger, D., S. Ehrt, M. I. Voskuil, Y. Liu, J. A. Mangan, I. M. Monahan, G. Dolganov, B. Efron, P. D. Butcher, C. Nathan, and G. K. Schoolnik. 2003. Transcriptional adaptation of *Mycobacterium tuberculosis* within macrophages: insights into the phagosomal environment. *J. Exp. Med.* **198**:693–704.
  49. Shimono, N., L. Morici, N. Casali, S. Cantrell, B. Sidders, S. Ehrt, and L. W. Riley. 2003. Hypervirulent mutant of *Mycobacterium tuberculosis* resulting from disruption of the *mce1* operon. *Proc. Natl. Acad. Sci. USA* **100**:15918–15923.
  50. Song, T., S. L. Dove, K. H. Lee, and R. N. Husson. 2003. RshA, an anti-sigma factor that regulates the activity of the mycobacterial stress response sigma factor SigH. *Mol. Microbiol.* **50**:949–959.
  51. Song, T., S. E. Song, S. Raman, M. Anaya, and R. N. Husson. 2008. Critical role of a single position in the  $-35$  element for promoter recognition by *Mycobacterium tuberculosis* SigE and SigH. *J. Bacteriol.* **190**:2227–2230.
  52. Stewart, G. R., L. Wernisch, R. Stabler, J. A. Mangan, J. Hinds, K. G. Laing, D. B. Young, and P. D. Butcher. 2002. Dissection of the heat-shock response in *Mycobacterium tuberculosis* using mutants and microarrays. *Microbiology* **148**:3129–3138.
  53. Talaat, A. M., S. K. Ward, C. W. Wu, E. Rondon, C. Tavano, J. P. Bannantine, R. Lyons, and S. A. Johnston. 2007. Mycobacterial bacilli are metabolically active during chronic tuberculosis in murine lungs: insights from genome-wide transcriptional profiling. *J. Bacteriol.* **189**:4265–4274.
  54. Talaue, M. T., V. Venketaraman, M. H. Hazbón, M. Peteroy-Kelly, A. Seth, R. Colangeli, D. Alland, and N. D. Connell. 2006. Arginine homeostasis in J774.1 macrophages in the context of *Mycobacterium bovis* BCG infection. *J. Bacteriol.* **188**:4830–4840.
  55. Voskuil, M. I., K. C. Visconti, and G. K. Schoolnik. 2004. *Mycobacterium tuberculosis* gene expression during adaptation to stationary phase and low-oxygen dormancy. *Tuberculosis (Edinburgh)* **84**:218–227.
  56. Walters, S. B., E. Dubnau, I. Kolesnikova, F. Laval, M. Daffe, and I. Smith. 2006. The *Mycobacterium tuberculosis* PhoPR two-component system regulates genes essential for virulence and complex lipid biosynthesis. *Mol. Microbiol.* **60**:312–330.
  57. Yang, Y. H., S. Dudoit, P. Luu, D. M. Lin, V. Peng, J. Ngai, and T. P. Speed. 2002. Normalization for cDNA microarray data: a robust composite method addressing single and multiple slide systematic variation. *Nucleic Acids Res.* **30**:e15.
  58. Zhu, L., S. Phadtare, H. Nariya, M. Ouyang, R. N. Husson, and M. Inouye. 2008. The mRNA interferases, MazF-mt3 and MazF-mt7 from *Mycobacterium tuberculosis* target unique pentad sequences in single-stranded RNA. *Mol. Microbiol.* **69**:559–569.